Modeling of energy storage materials

D. Aksyonov, A. Boev, S. Fedotov, A. Zhugayevych, K. Stevenson, A. Abakumov
Center for Energy Science and Technology, Skoltech

Outline

1. Motivation to study energy materials and introduction into battery components

2. Modeling of solid electrodes

3. Modeling of electrolytes and interfaces

4. High-throughput modeling

5. Few examples from our experience: OH defects in $LiFePO_4$, antisite defects in layered oxides, migration barriers in cathodes

More than 1 billion gasoline cars on Earth

Gas chamber for execution:

Solution: renewables and electric cars

- Renewable electricity is unpredictable
- Electric cars - the range is limited - the price is high
- Both currently are economically unreasonable

What can change the situation?

Affordable energy storage!

Energy storage technologies

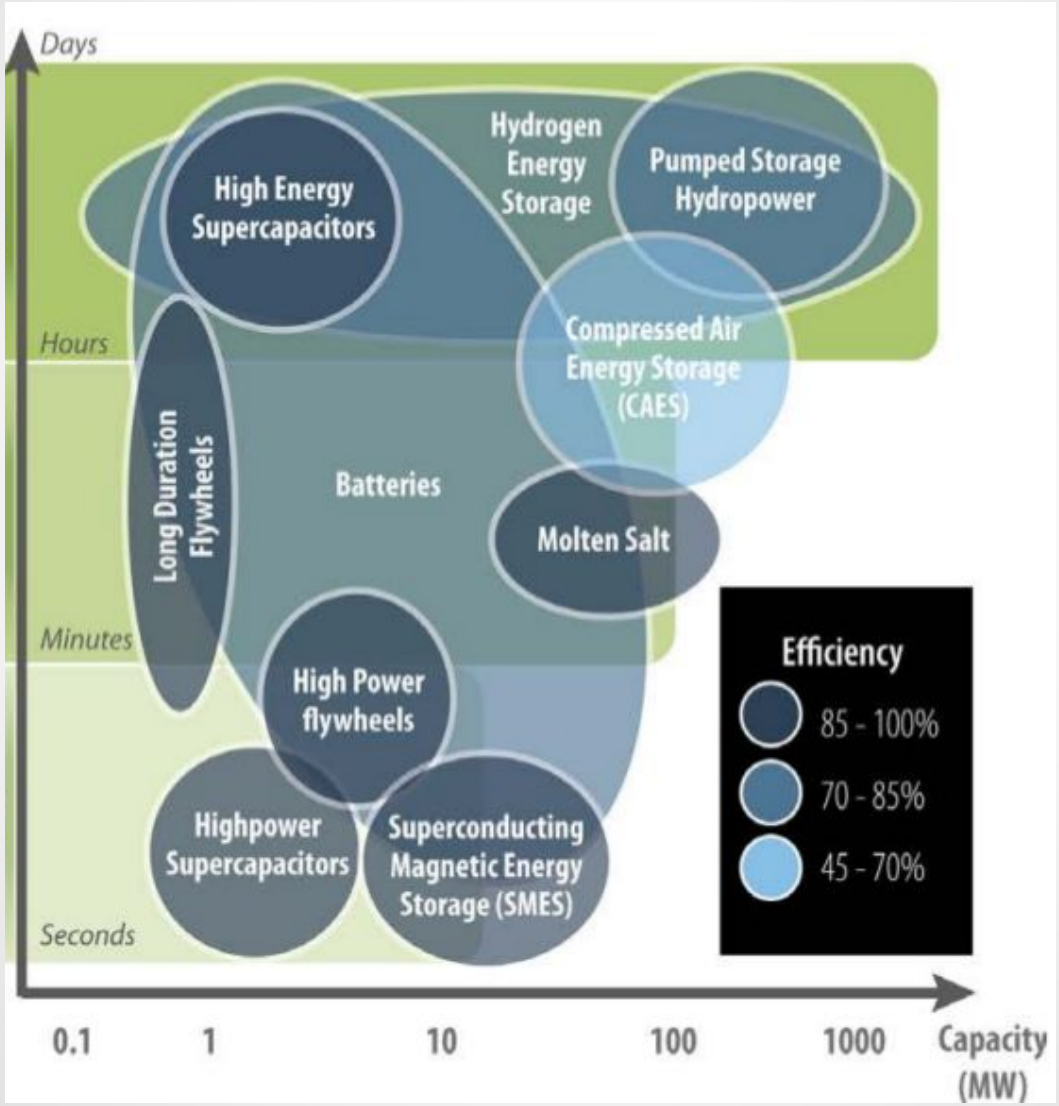

Among energy storage technologies Li-ion is the main for portable electronics, cars, and even grid storage

The best known advocate for Li-ion is Tesla

Model 3 up to
500 000 cars in 2020

Tesla heavy Truck

Tesla Energy Solar + Li-ion

How the metal-ion battery works

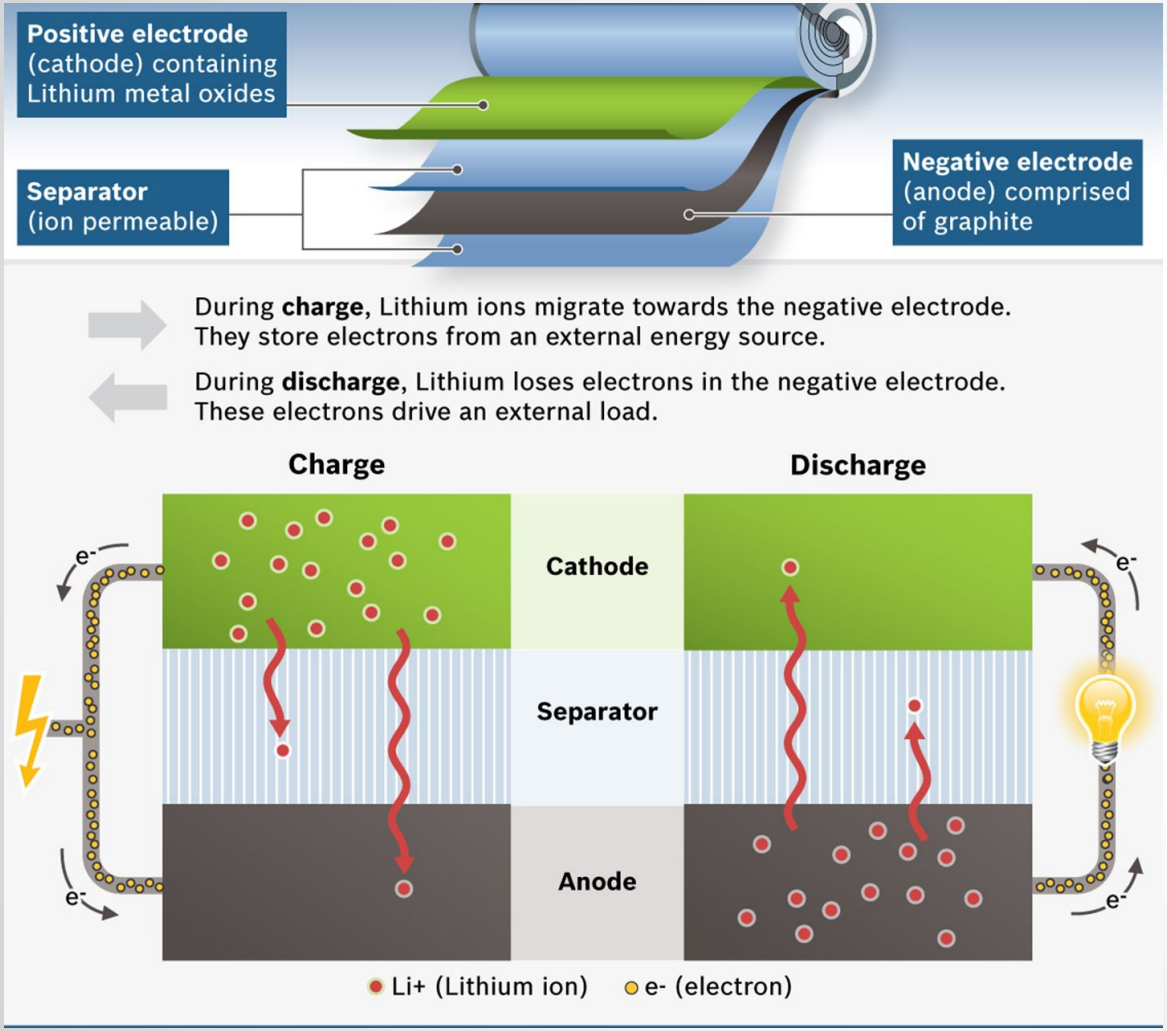

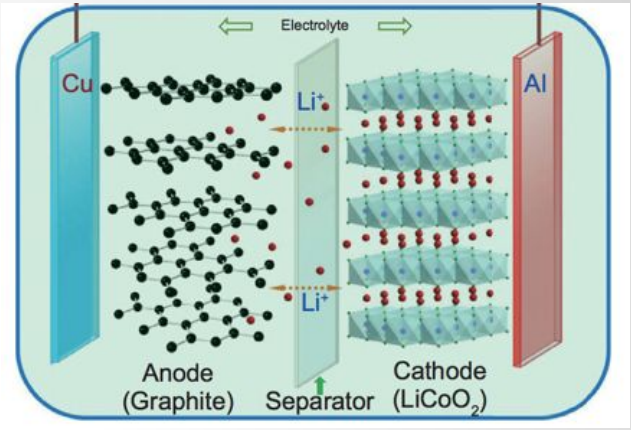

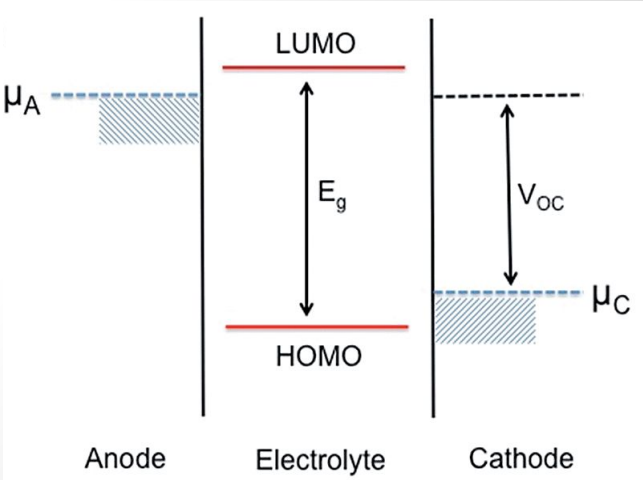

6C <-> LiC_6

$LiCoO_2$ <-> CoO_2

Important battery metrics

Metric	Depends on
Voltage (V)	Chemistry and structure of cathode and anode, working window of electrolyte
Capacity (C)	Chemistry and structure of cathode and anode
Energy density	$E = \int V(C)dC$
Safety	Thermodynamical stability of cathode, anode, and electrolyte, battery construction
Power density	Ionic and electronic conductivity of cathode and anode

Both anode and cathodes are important! In our work we study cathodes

Main classes of cathode materials

CoO_6 octahedra

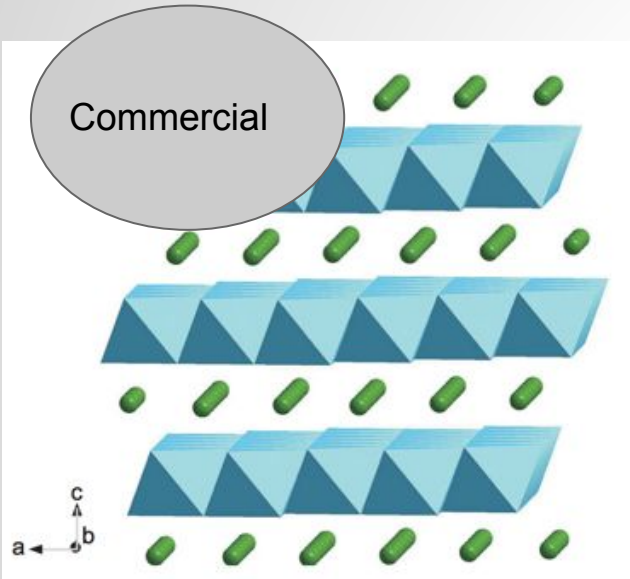

$LiCoO_2$, $NaCoO_2$
Layered oxides,
Transition metals are
Co, Mn, Ni
good for Li and Na

FeO_6 octahedra
PO_4 tetrahedra

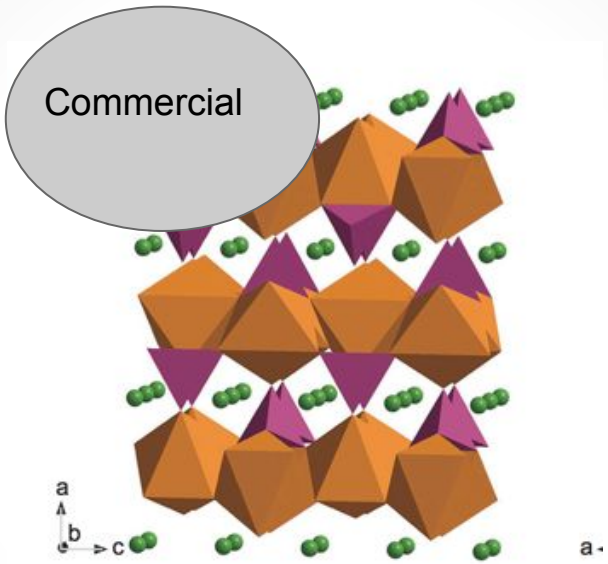

$LiFePO_4$, $NaFePO_4$
Olivines
High stability

VO_6
octahedra

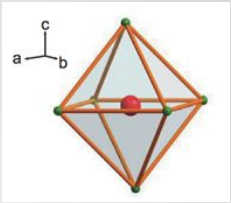

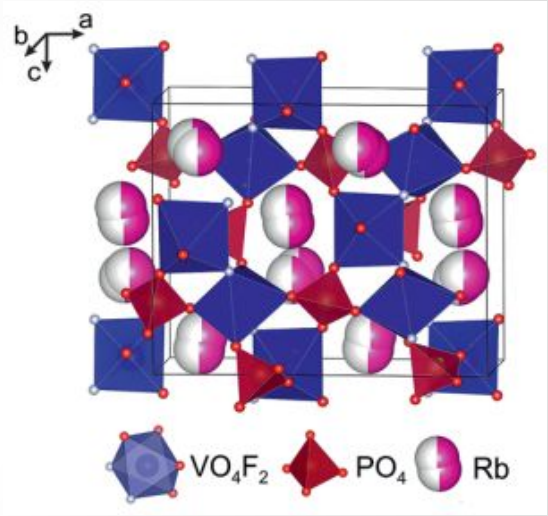

Other polyanion
materials, e.g.
$KVPO_4F$, Na_2FePO_4F,
etc. SO_4, SiO_4, BO_3
polyanion Li, Na and K

Anode materials

Graphite

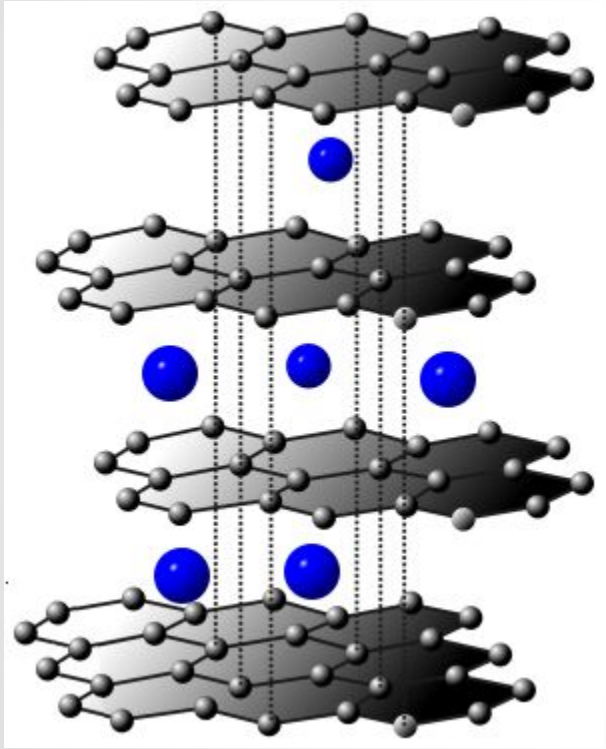

Anatase, $LiTiO_2$

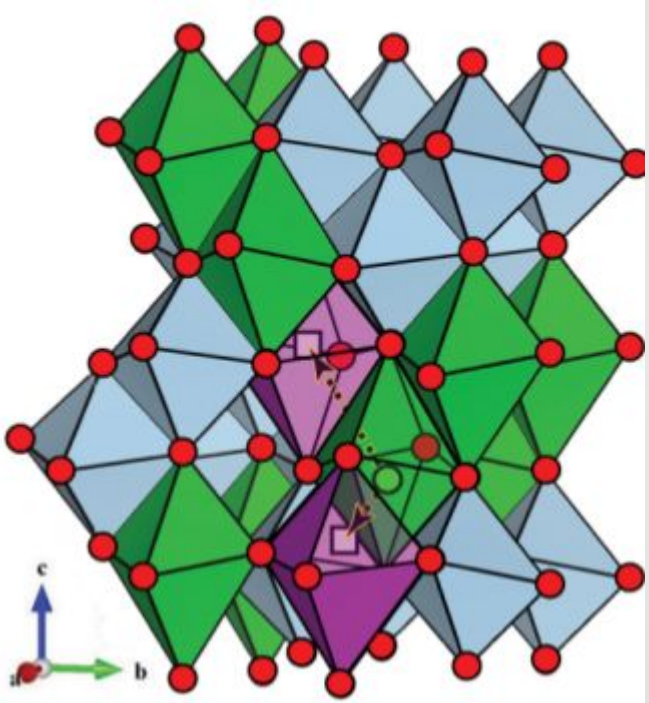

Electrolytes: liquid and solid

Li salts, such as $LiPF_6$ in organic solvents such as ethylene carbonate, propylene carbonate, etc

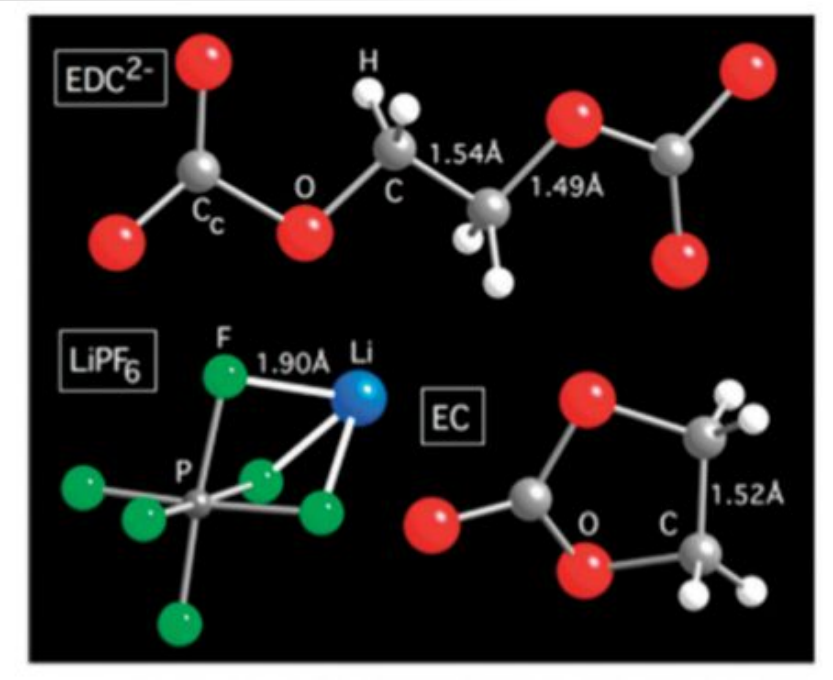

Solid electrolytes

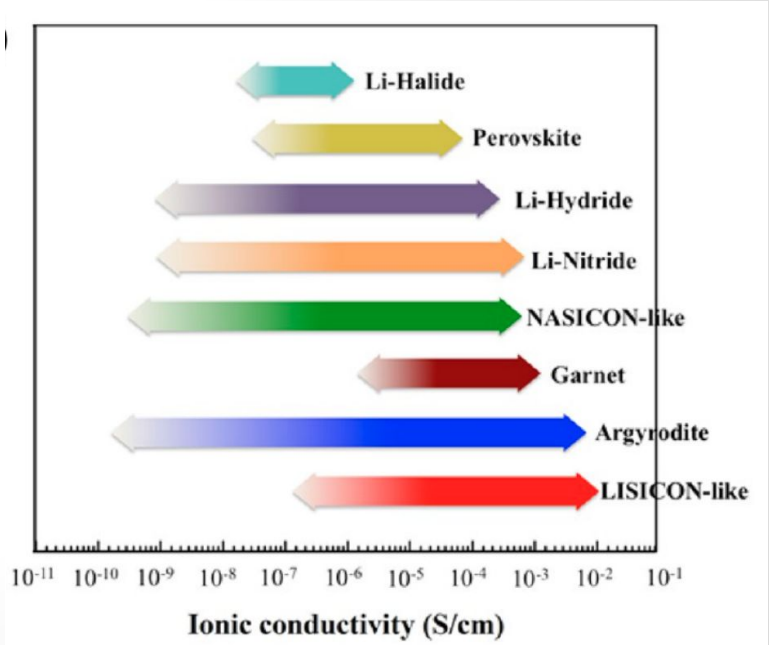

Meesala, Yedukondalu, et al. "Recent advancements in Li-ion conductors for all-solid-state Li-ion batteries." *ACS Energy Letters* 2.12 (2017): 2734-2751.

Outline

1. Motivation to study energy materials and introduction into battery components

2. Modeling of solid electrodes

3. Modeling of electrolytes and interfaces

4. High-throughput modeling

5. Few examples from our experience: OH defects in $LiFePO_4$, antisite defects in layered oxides, migration barriers in cathodes

Modeling of battery materials

Cathodes, anodes, solid state conductors:

- Phase stability (DFT+U)
- Intercalation voltages and intercalation mechanism (DFT+U, Hybrid)
- Diffusivity of cations (DFT+U, MD)
- Defects and influence on properties(DFT+U)

Liquid electrolytes (DFT, MD):

- Solvation energies (MP2, CI, CC, DFT)
- Electrolyte stability (MP2, CI, CC, DFT)

Li-Fe-P-O phase diagram, $\mu(O_2) = -12.4$ eV

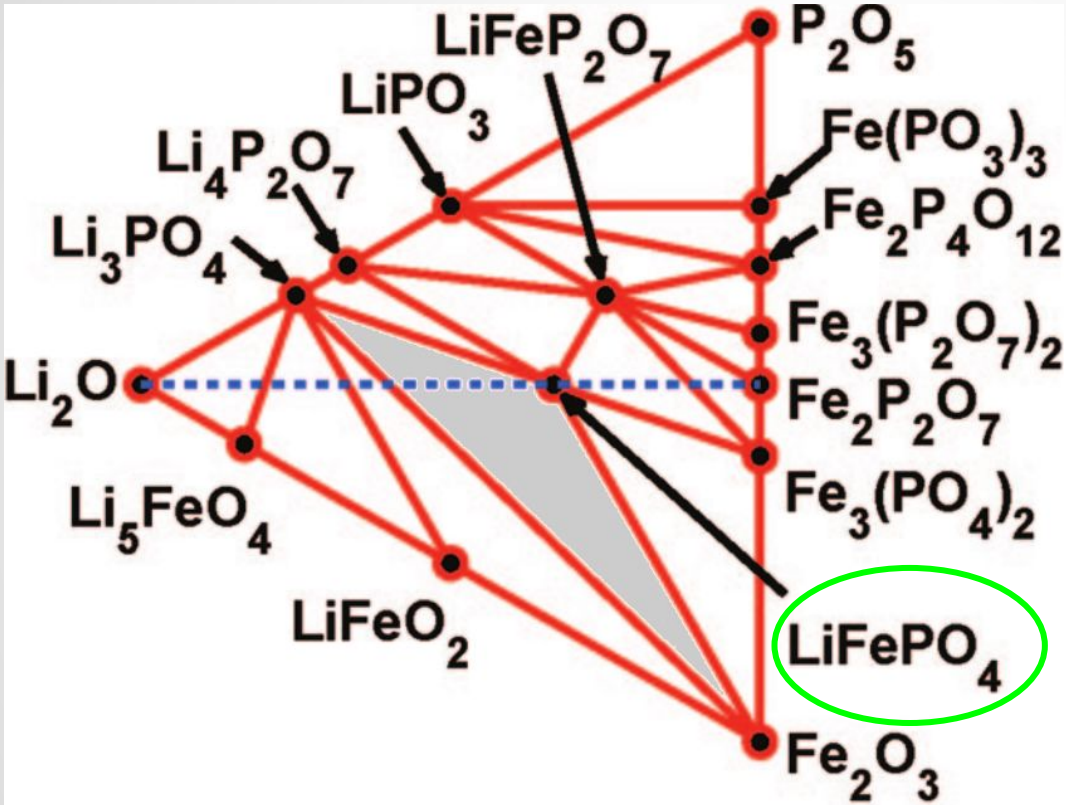

$$\overline{\varphi}(\mu_{O_2}, x_{Li}, x_{Fe}, x_P) \approx \frac{E - \mu_{O_2} N_{O_2}}{N_{Li} + N_{Fe} + N_P}$$

1. Ong, S.P., Wang, L., Kang, B. and Ceder, G. Li–Fe–P–O2 Phase Diagram from First Principles Calculations. Chemistry of Materials. 20, 5 (Mar. 2008), 1798–1807.

Average intercalation voltage

$$\overline{V}(x_1, x_2) \approx -\frac{E(\mathrm{Li}_{x_1}\mathrm{MO}_2) - E(\mathrm{Li}_{x_2}\mathrm{MO}_2) - (x_1 - x_2)\, E(\mathrm{Li})}{(x_1 - x_2)\, F}$$

with $x_1 > x_2$,

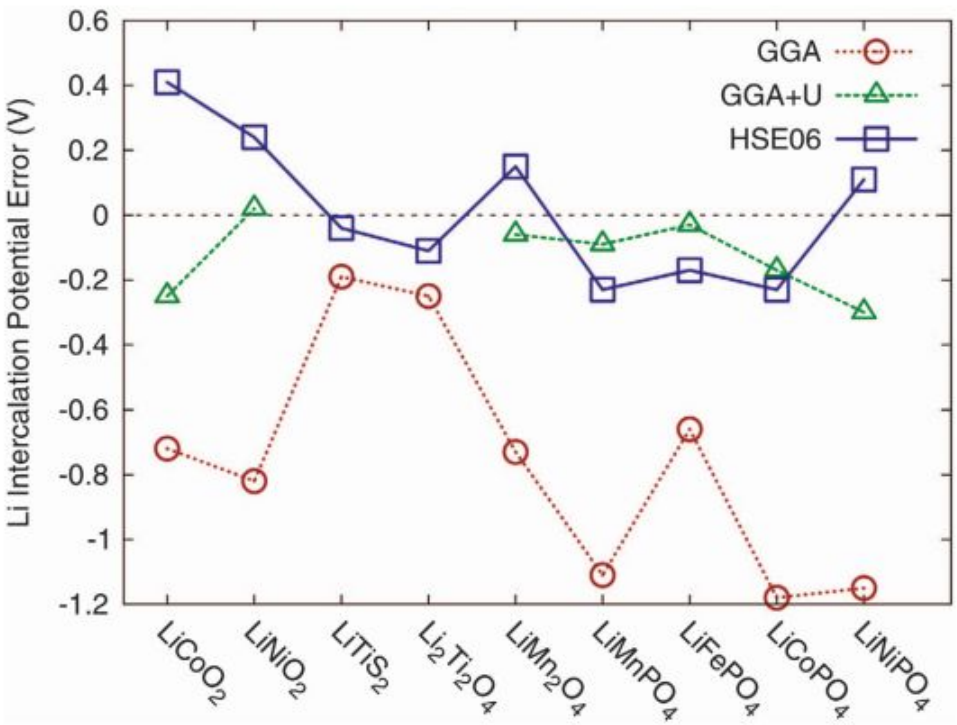

Urban, A. et al.// *npj Computational Materials* 2.1 (2016): 1-13.

DFT+U calculations

x_1 = 100 %, x_2 = 0 %

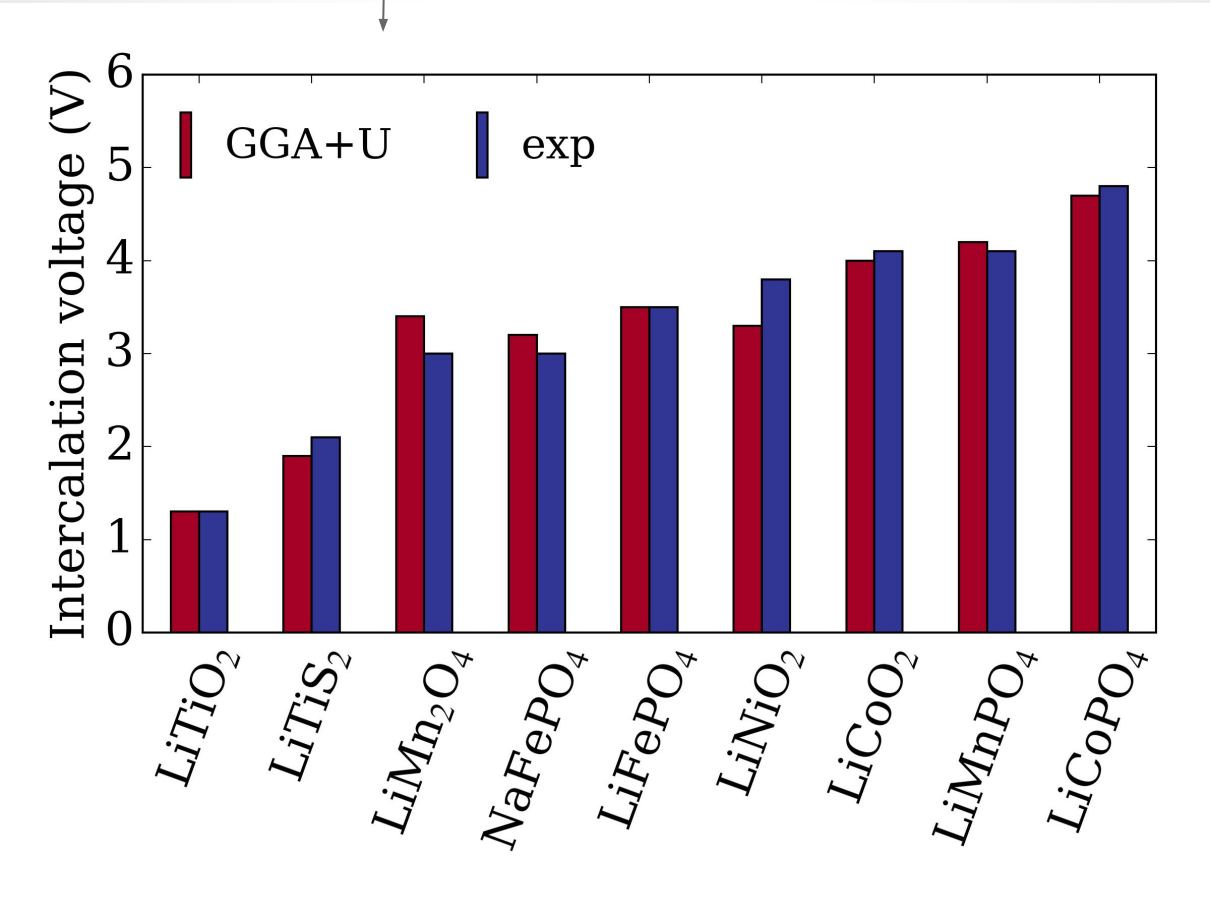

Voltage profile NaCoO2 (P2)

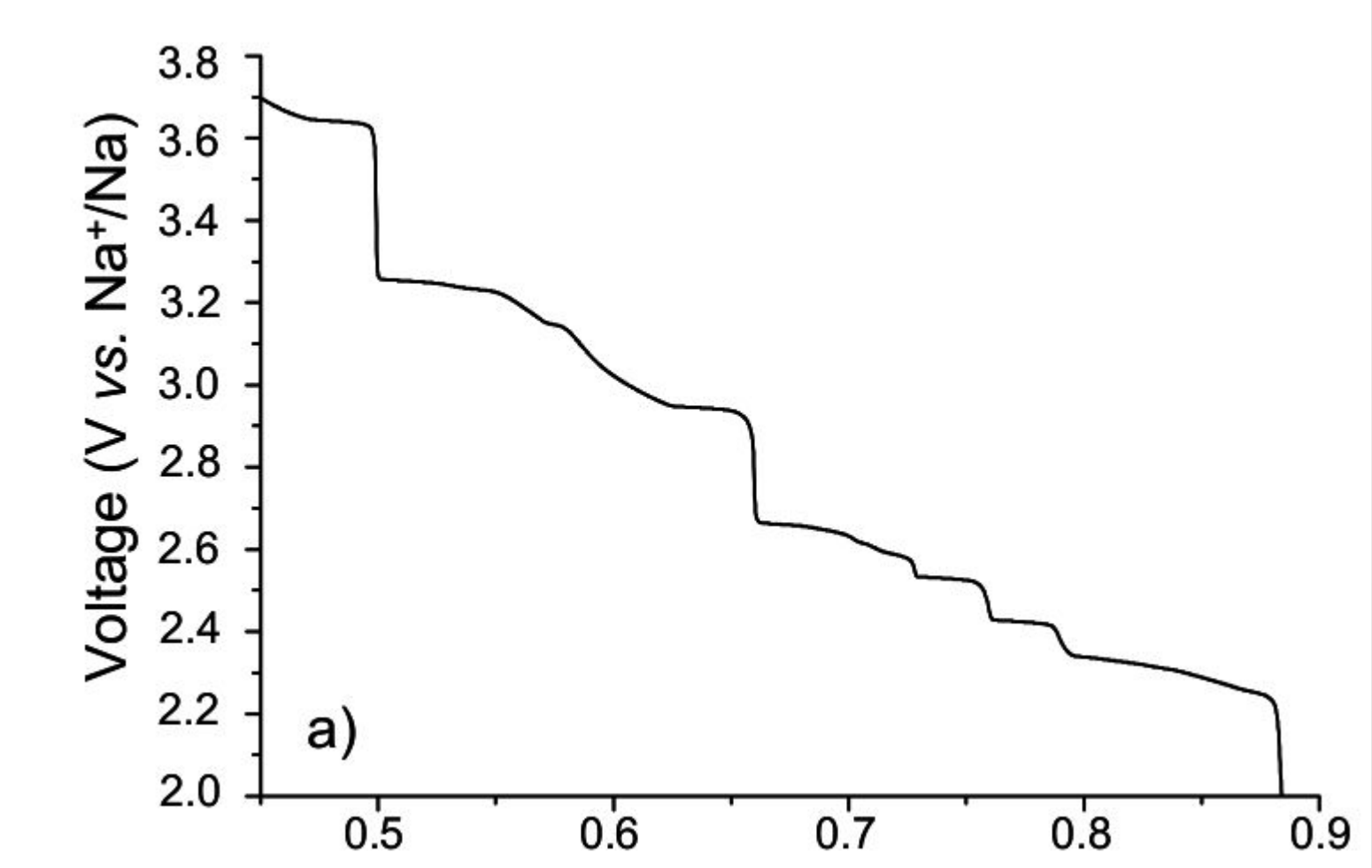

berthelot2011_SI_nature

Calculation of voltage profiles

$$E_f(Li_xMO_2) = E(Li_xMO_2) - x\,E(LiMO_2) - (1-x)\,E(MO_2),$$

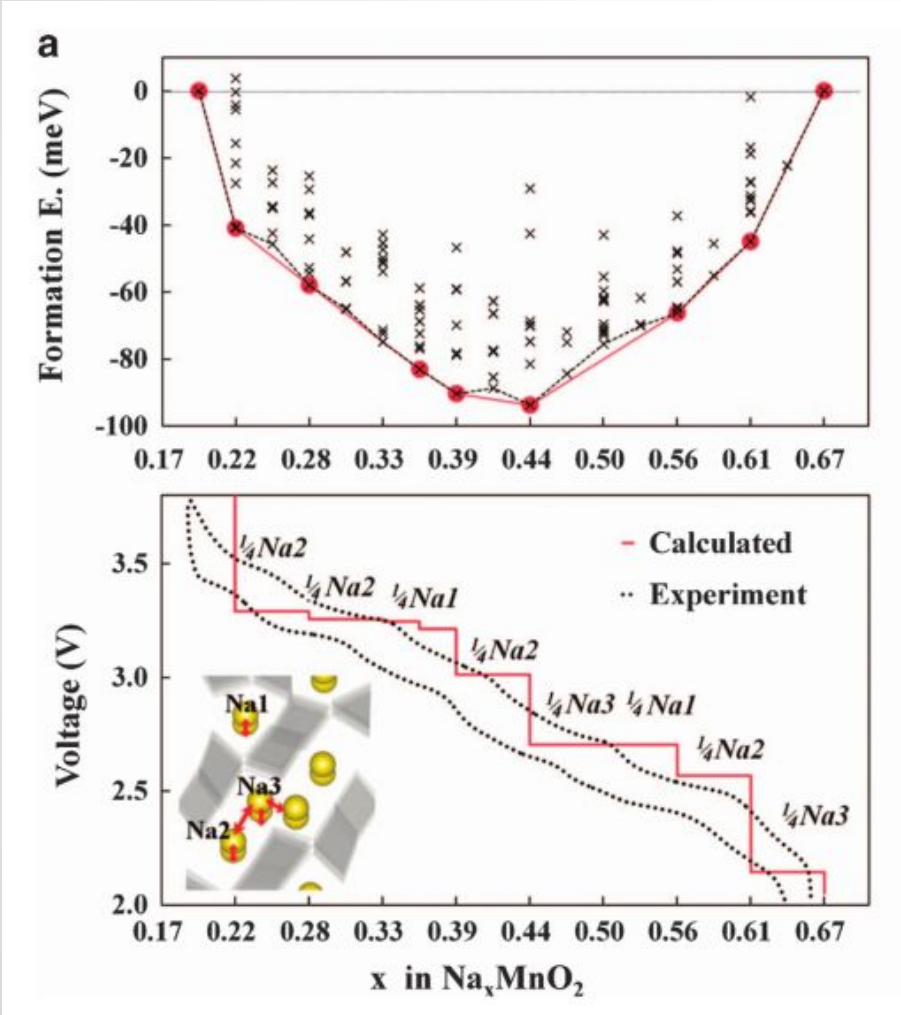

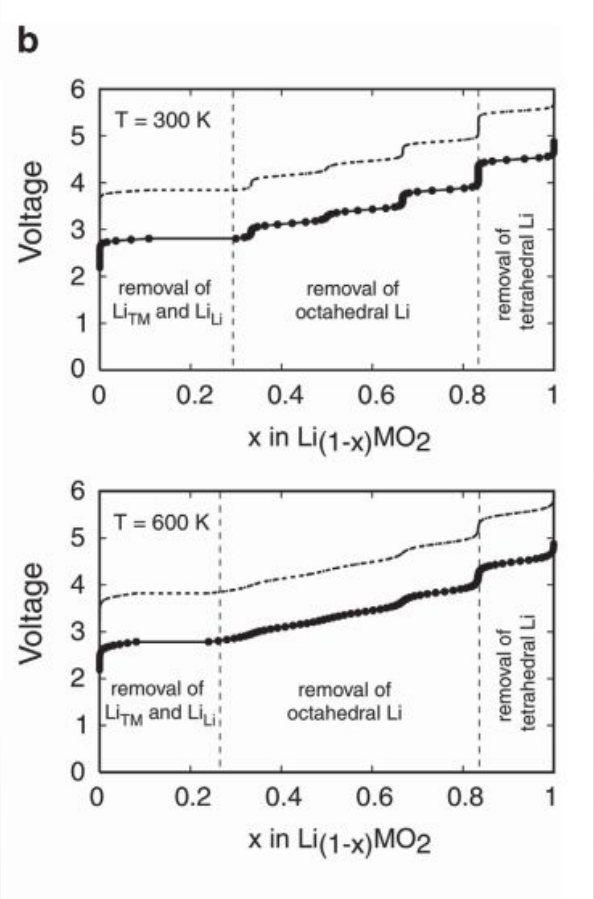

Urban, A. et al.// *npj Computational Materials* 2.1 (2016): 1-13.

Thermal stability of electrode

$$Li_xM_yO_{z+z'} \rightarrow Li_xM_yO_z + \frac{z'}{2}O_2,\ \Delta G_r \approx E(Li_xM_yO_z) + \frac{z'}{2}E^*(O_2) - E(Li_xM_yO_{z+z'}) - \frac{z'}{2}TS_{O_2}^{p_0}(T),$$

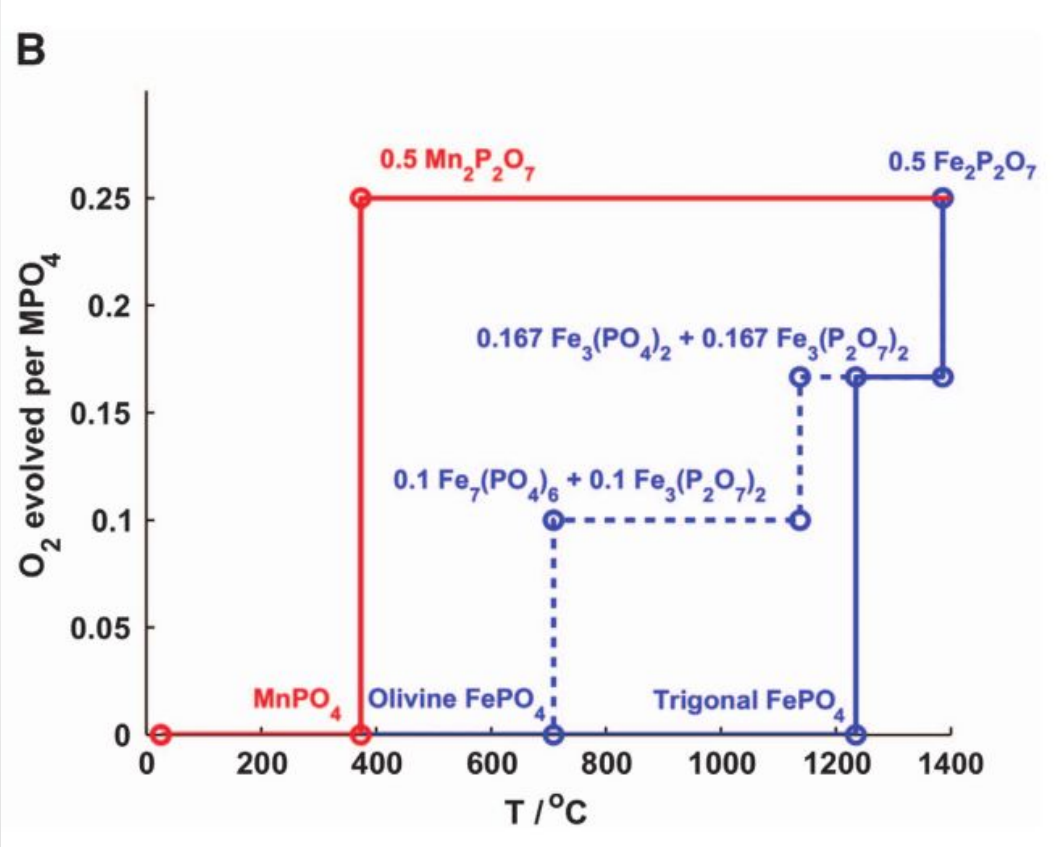

Urban, A. et al.// *npj Computational Materials* 2.1 (2016): 1-13.

Main errors in DFT+U for calculating formation energies of cathode materials

(i) a constant energy shift of the DFT O_2 energy to account for overbinding fixed by constant correction

(ii) a Hubbard U correction

using U values fitted to experimental oxide formation energies error in the formation energies of transition-metal oxides from up to 1.0 eV with GGA to less than 0.1 eV in most cases.

Urban, A. et al.// *npj Computational Materials* 2.1 (2016): 1-13.

Typical galvanostatic curve at different C-rates shows diffusion limitation

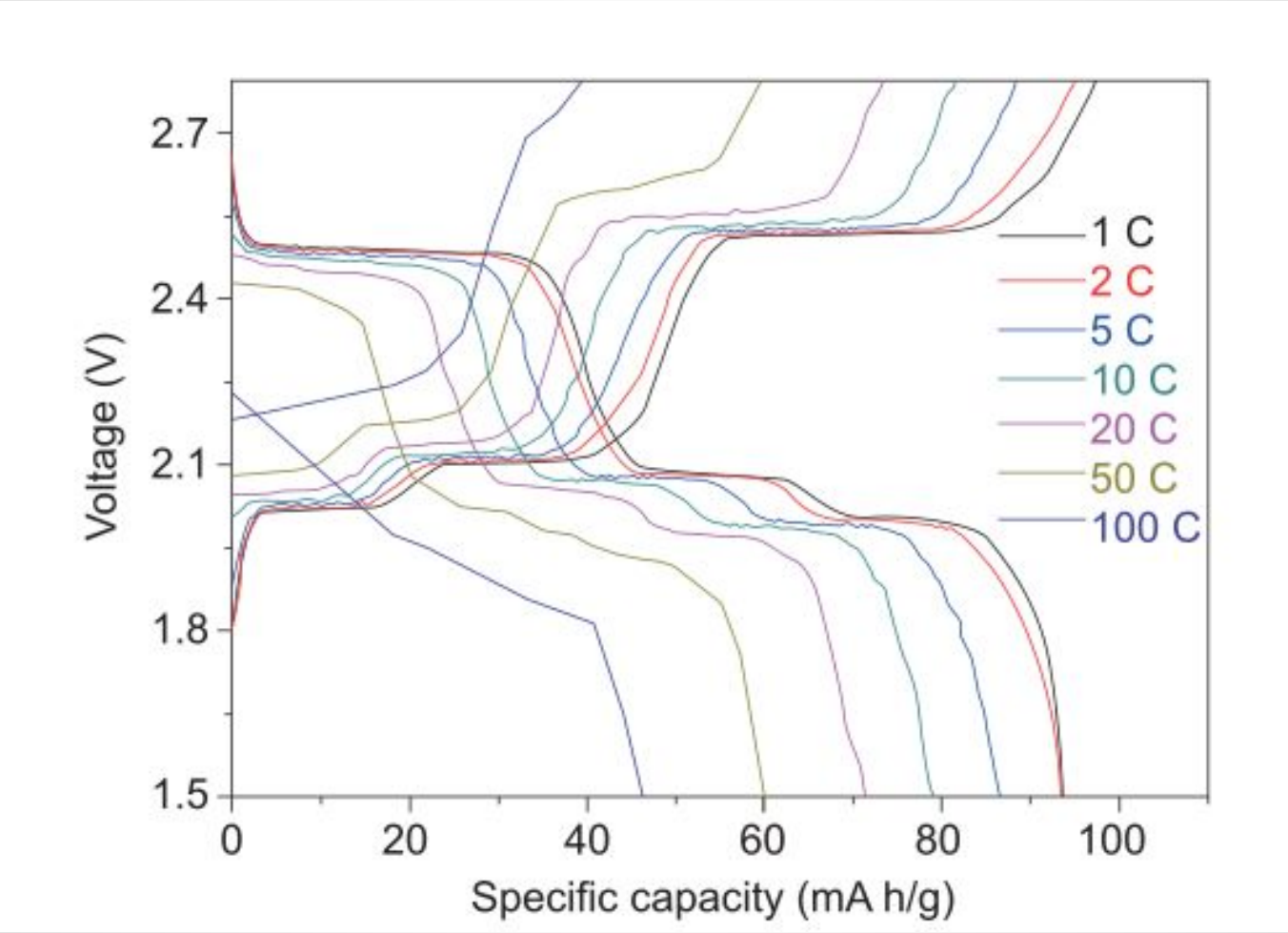

LVP//LTO battery

Massé, Robert C., et al. "Energy storage through intercalation reactions: electrodes for rechargeable batteries." *National Science Review* 4.1 (2017): 26-53.

Ionic conductivity, Ab initio MD

Li trajectories in $Li_{10}GeP_2S_{12}$ at 900 K

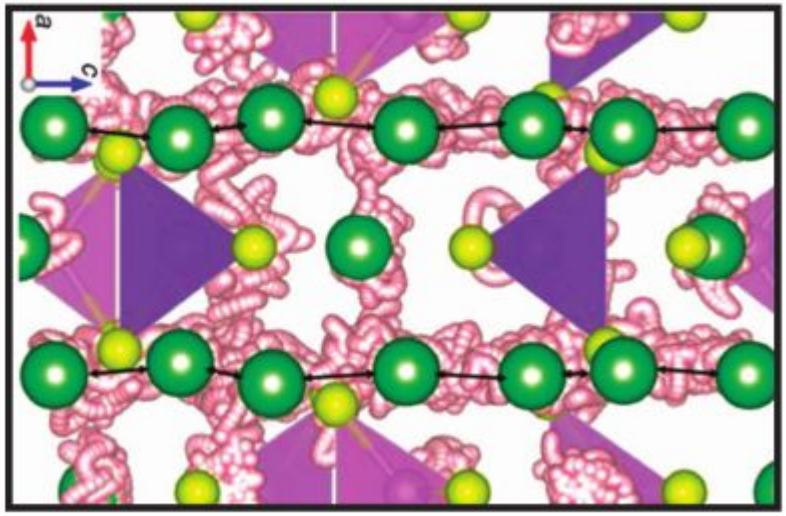

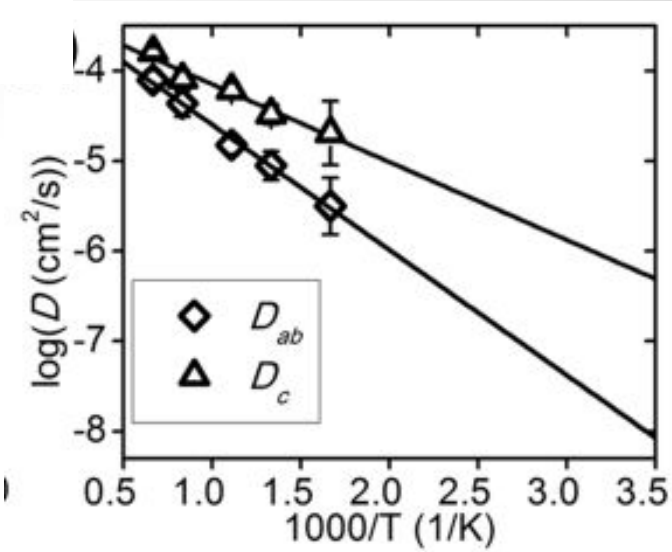

$$D(T) \approx D_0 \; e^{-\frac{E_a}{k_B T}},$$

$$\sigma(T) = \frac{N_{Li} \; e^2}{V \; k_B \; T} \; D(T),$$

Arrhenius law: E_a is activation energy for diffusion

Nernst–Einstein relation for ionic conductivity. N_{Li} is the number of lithium ions, V is the volume of the simulation cell

Urban, A. et al.// *npj Computational Materials* 2.1 (2016): 1-13.

Mo, Yifei, Shyue Ping Ong, and Gerbrand Ceder. " *Chemistry of Materials* 24.1 (2012): 15-17.

Diffusivity based on 0 K migration barriers

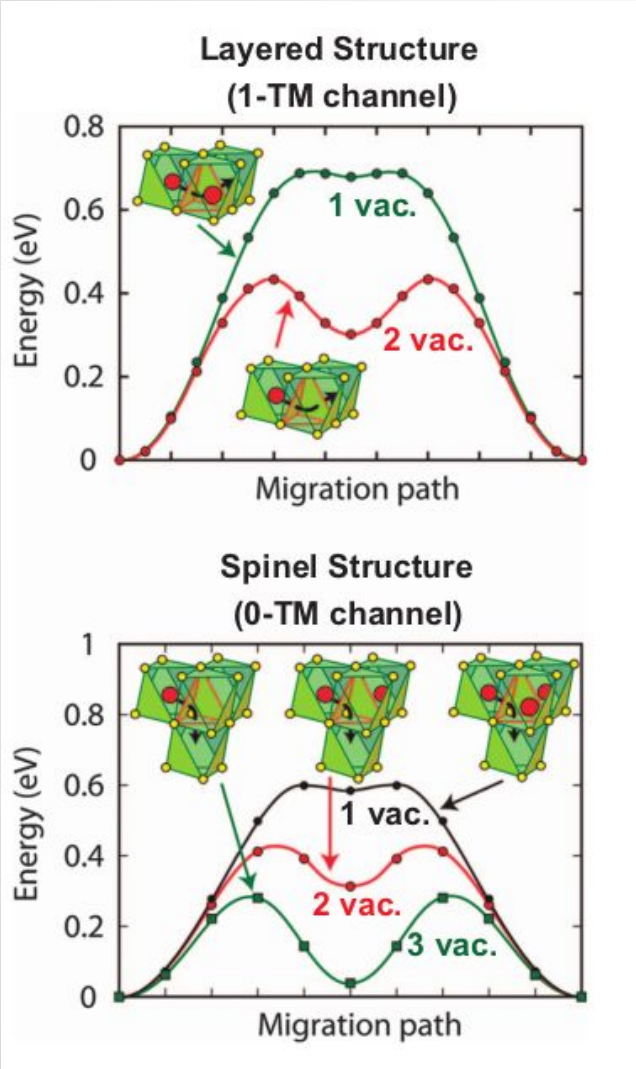

Rate of the hopping process

$$k(T) = \nu^*(T)\, e^{-\frac{\Delta G^{\ddagger}(T)}{k_B T}},$$

v* is temperature-dependent effective attempt frequency, ΔG ‡ is Gibbs free energy of activation (migration barrier)

$$D \approx g \cdot a^2 \cdot k,$$

a is hopping distance, g is geometrical factor (~1)

Typical values for the prefactor v* are 10^{11} to 10^{13} s^{-1}

NEB method for finding saddle points

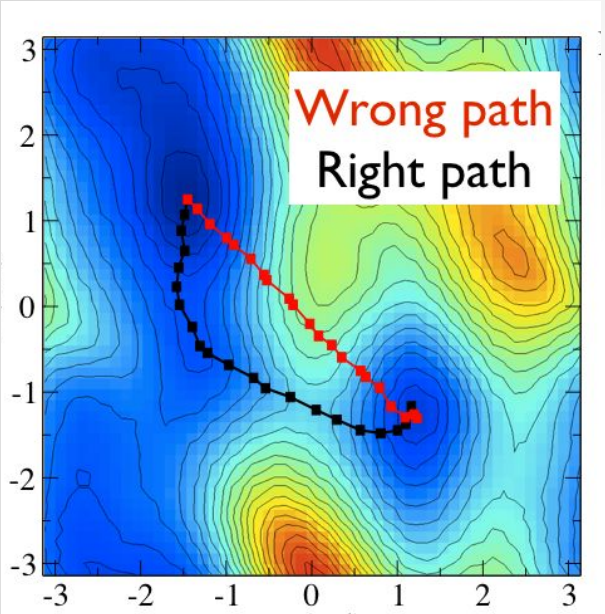

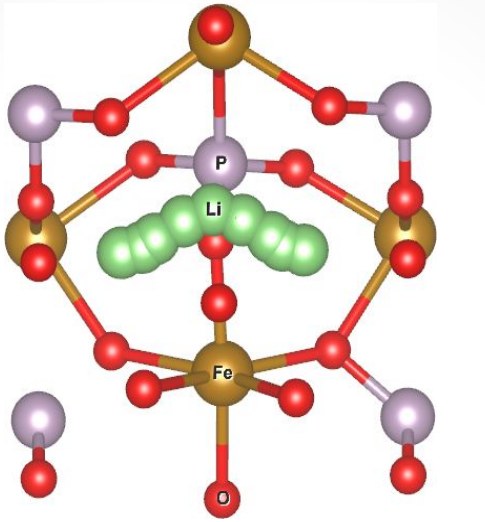

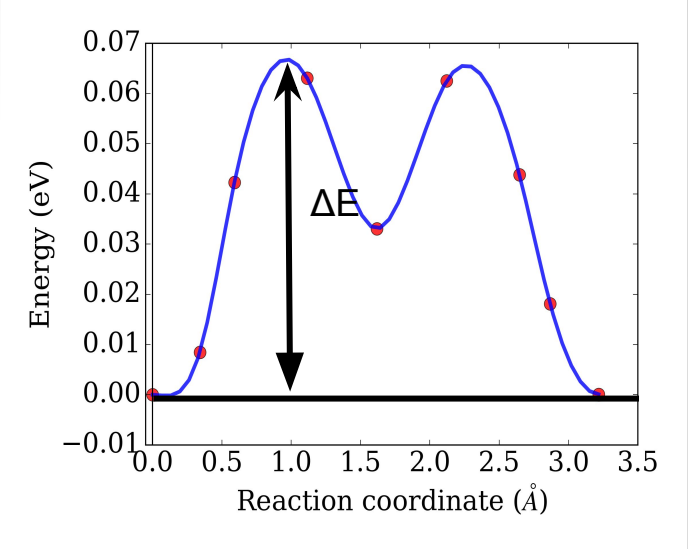

Nudged elastic band method (**NEB**) is used to find minimum energy paths and migration barriers at saddle points.

The spring forces keep the images spaces equally, allowing to propagate a chain towards minimum energy path.

Outline

1. Motivation to study energy materials and introduction into battery components

2. Modeling of solid electrodes

3. Modeling of electrolytes and interfaces

4. High-throughput modeling

5. Few examples from our experience: OH defects in $LiFePO_4$, antisite defects in layered oxides, migration barriers in cathodes

Modeling of electrolyte

Solvent	Structure	M. Wt	T_m/°C	T_b/°C	η/cP 25 °C	ε 25 °C
EC	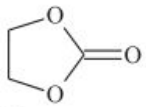	88	36.4	248	1.90 (40 °C)	89.78
PC	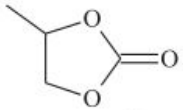	102	−48.8	242	2.53	64.92

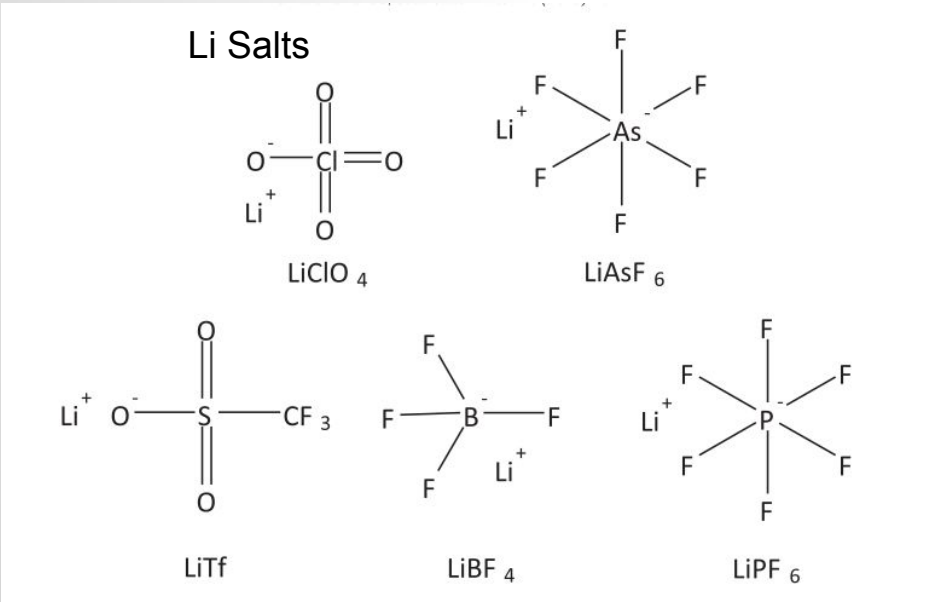

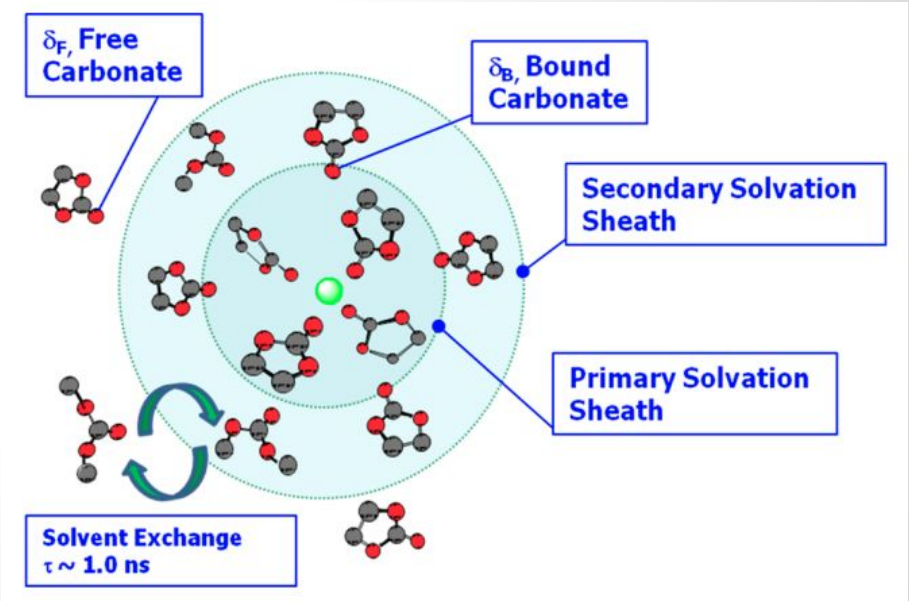

Marcinek, M., et al. *Solid State Ionics* 276 (2015): 107-126.

Bogle, X, et al. *The journal of physical chemistry letters* 4.10 (2013): 1664-1668.

Electrochemical stability of electrolytes

$$\text{reduction}: \quad \Delta G^{s}_{red} = G[M^{n-}(s)] - G[M(s)] - nG[e^{-}(s)]$$
$$\text{oxidation}: \quad \Delta G^{s}_{ox} = G[M^{n+}(s)] + nG[e^{-}(s)] - G[M(s)],$$

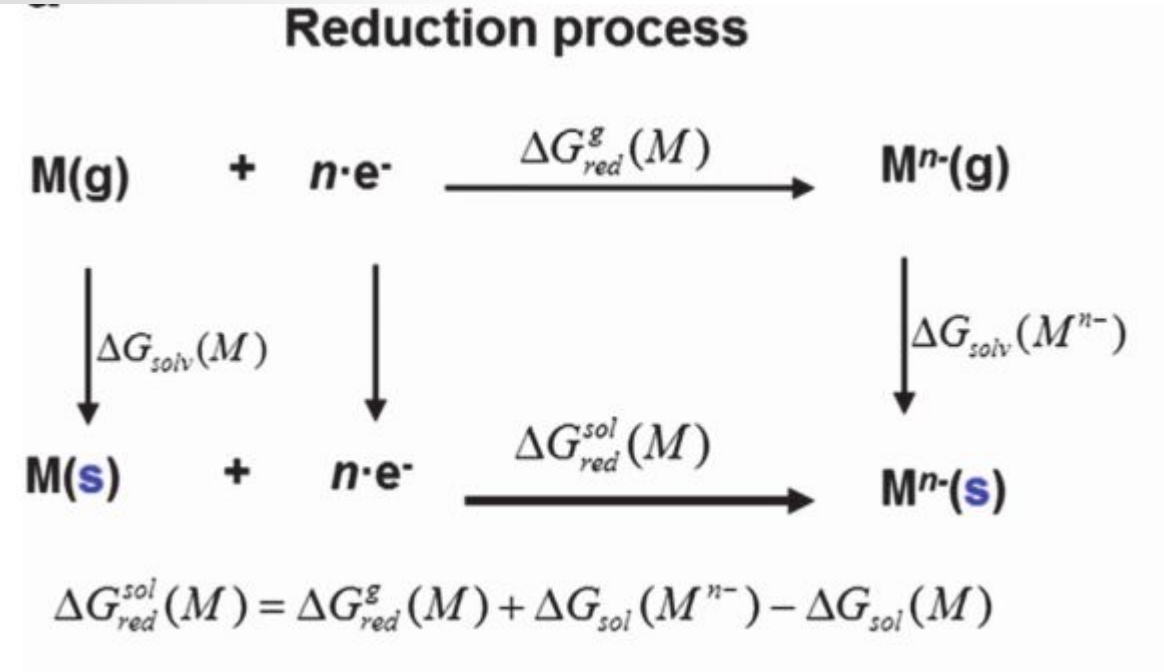

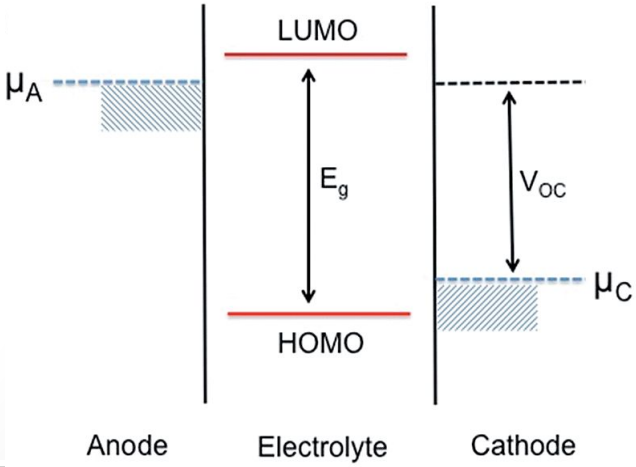

Zhang, X*Journal of The Electrochemical Society* 148.5 (2001): E183-E188.

HOMO and LUMO for screening electrolytes

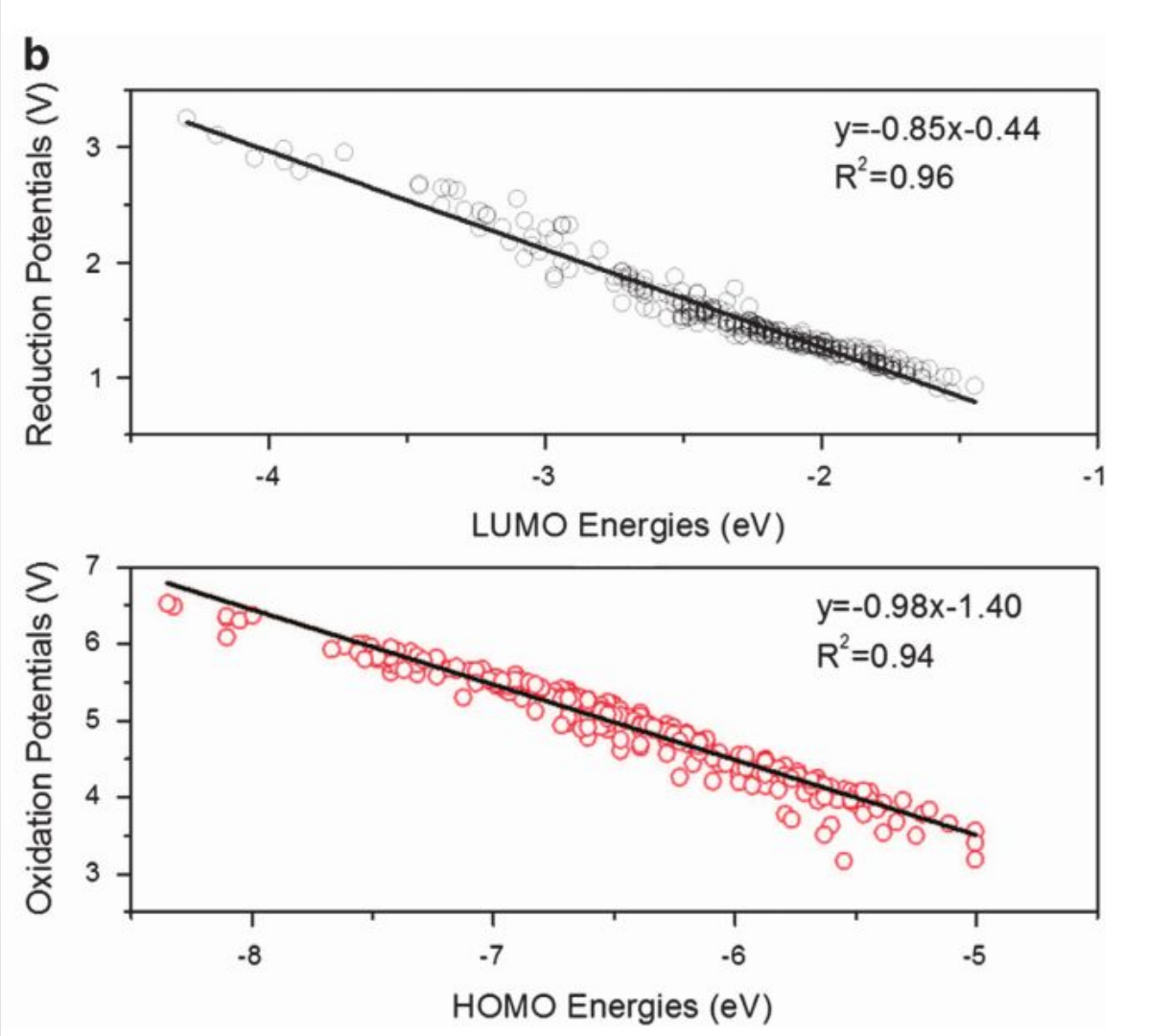

Cheng, L, et al. " *The journal of physical chemistry letters* 6.2 (2015): 283-291.

Electrolyte/electrode interface the largest challenge for modelling now

Diffusion is only half of the story, kinetics of interphase charge transfer is highly important

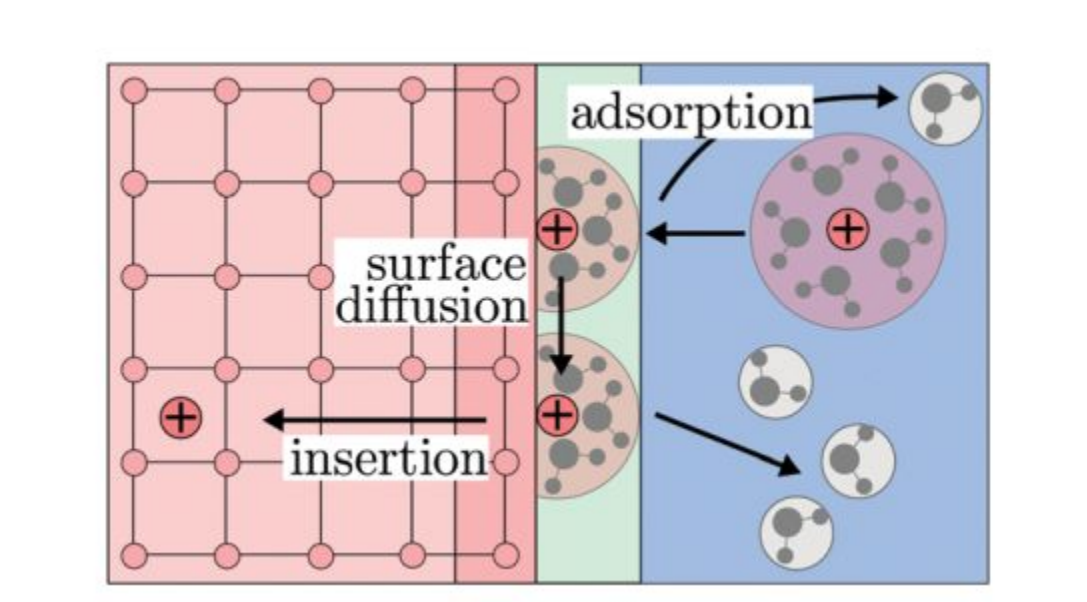

Li, Yunsong, and Yue Qi. "Energy landscape of the charge transfer reaction at the complex Li/SEI/electrolyte interface." *Energy & Environmental Science* 12.4 (2019): 1286-1295.

Lück, Jessica, and Arnulf Latz. "Modeling of the electrochemical double layer and its impact on intercalation reactions." *Physical Chemistry Chemical Physics* 20.44 (2018): 27804-27821.

Outline

1. Motivation to study energy materials and introduction into battery components

2. Modeling of solid electrodes

3. Modeling of electrolytes and interfaces

4. High-throughput modeling

5. Few examples from our experience: OH defects in $LiFePO_4$, antisite defects in layered oxides, migration barriers in cathodes

What is high-throughput (HT) computational materials design?

- the amount of data is way too high to be produced or analyzed by direct intervention of researcher - therefore must be performed automatically
- the results are stored in database, which is further analyzed for selecting novel materials or gaining new physical insights

The next step and a revolution in computational materials design!

High-throughput computational screening of new Li-ion battery anode materials

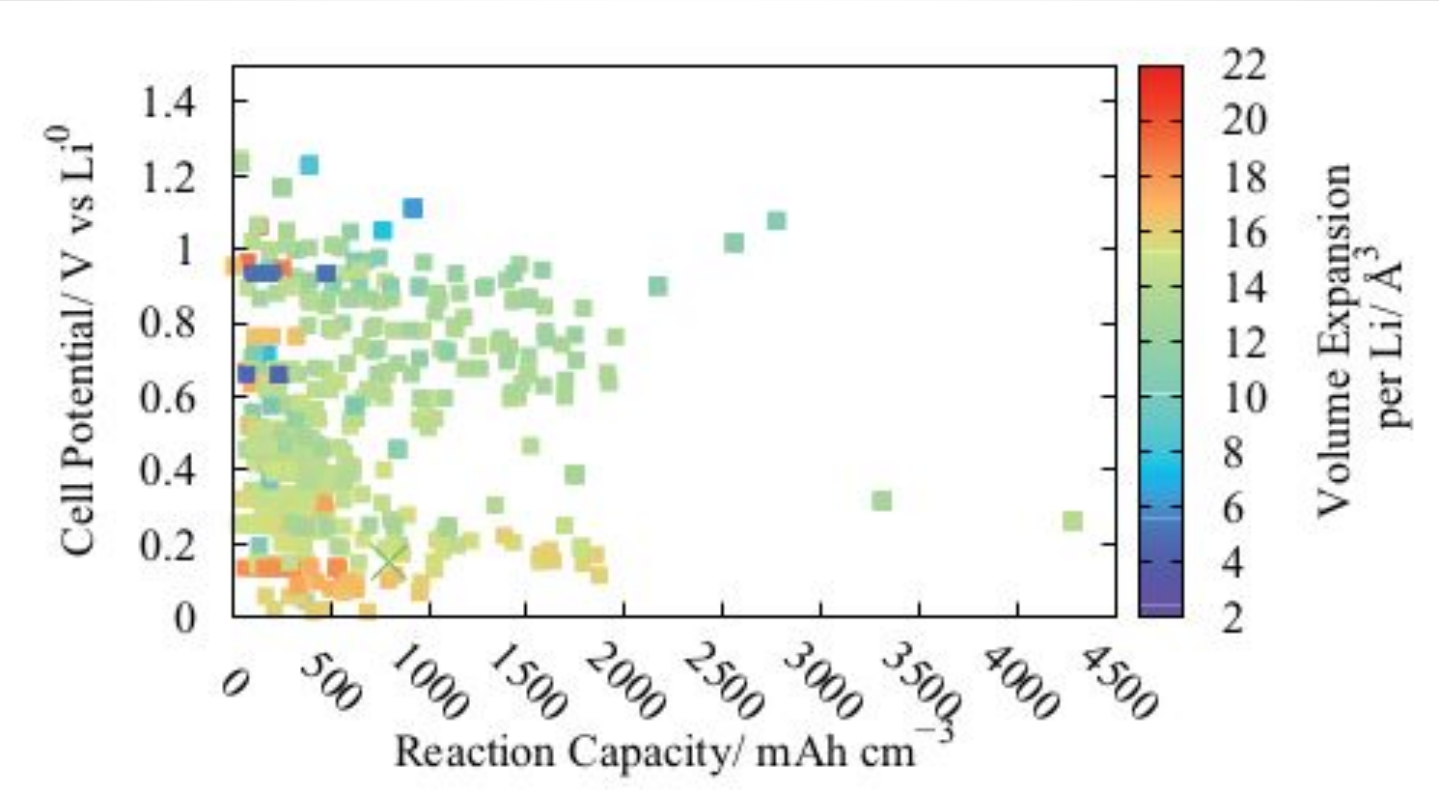

Kirklin, Scott, Bryce Meredig, and Chris Wolverton. "High-throughput computational screening of new Li-ion battery anode materials." *Advanced Energy Materials* 3.2 (2013): 252-262.

High-throughput Electrolyte discovery

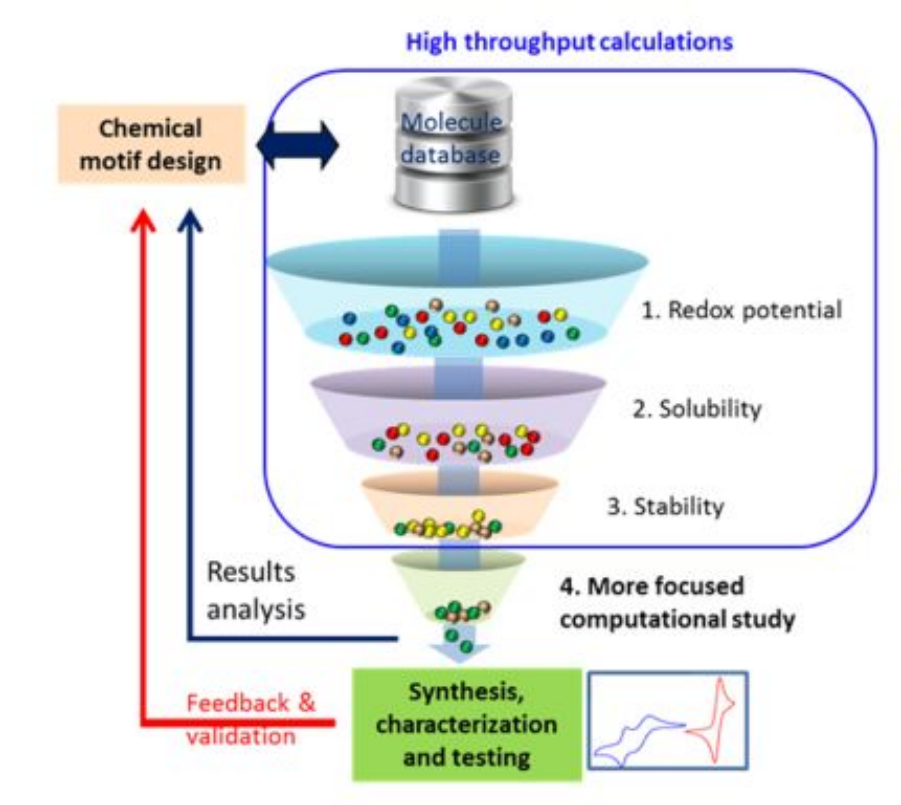

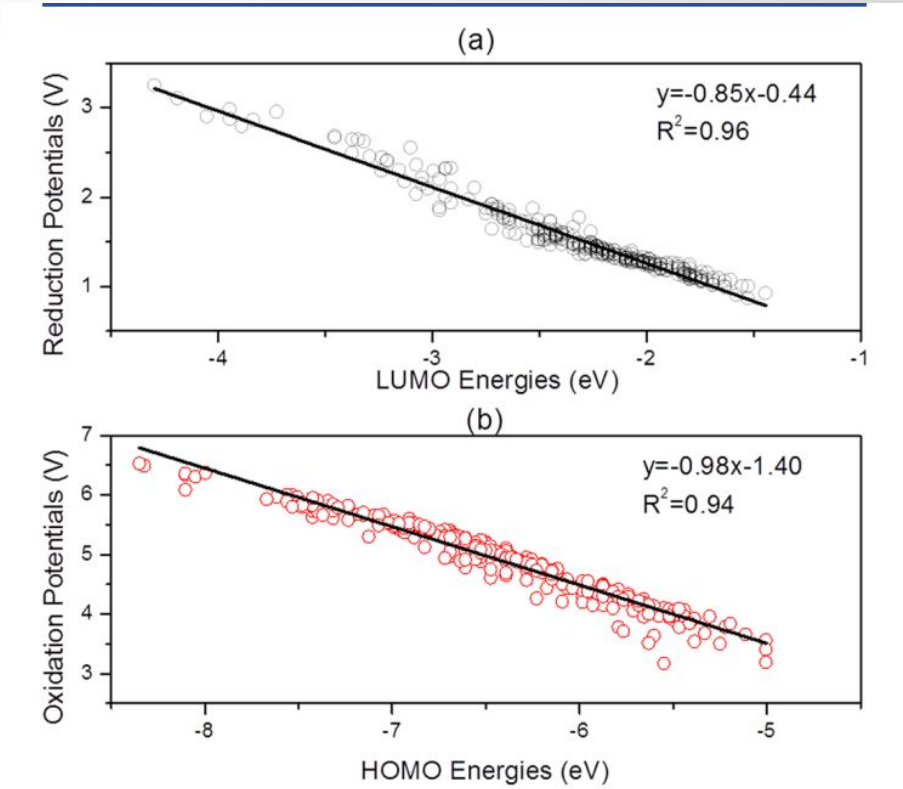

Cheng, Lei, et al. "Accelerating electrolyte discovery for energy storage with high-throughput screening." *The journal of physical chemistry letters* 6.2 (2015): 283-291.

Screening of Cathode Coatings for Solid-State Batteries

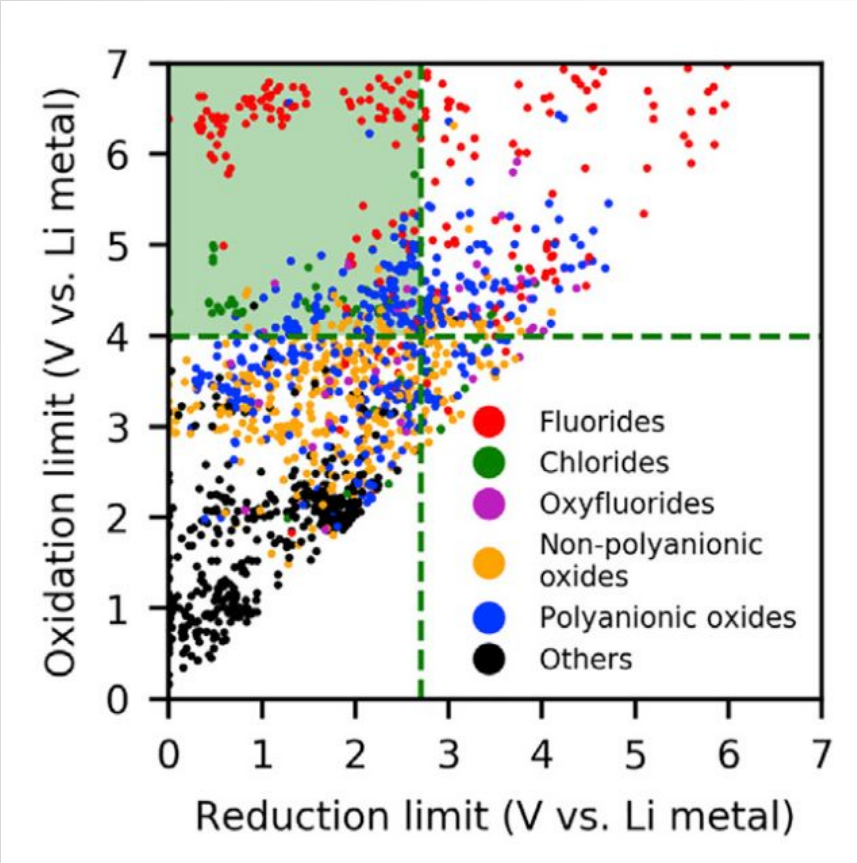

Coatings	ICSD #	Calculated Migration Barrier (eV)	Experimental Activation Energy (eV)
Li_2ZrO_3	31941	0.48	0.5,[77] 0.68[78]
LiH_2PO_4	100200	0.33	–[a]
$LiTi_2(PO_4)_3$	95979	0.42	0.47[79]
$LiBa(B_3O_5)_3$	93013	1.96	–
$LiPO_3$	51630	0.40	1.40[82]
$LiLa(PO_3)_4$	416877	1.39	0.92[b81]
$LiCs(PO_3)_2$	62514	1.27	1.31[80]

Xiao, Yihan, et al. "Computational screening of cathode coatings for solid-state batteries." *Joule* 3.5 (2019): 1252-1275.

Screening of more than 12 000 candidates for solid lithium-ion conductor materials

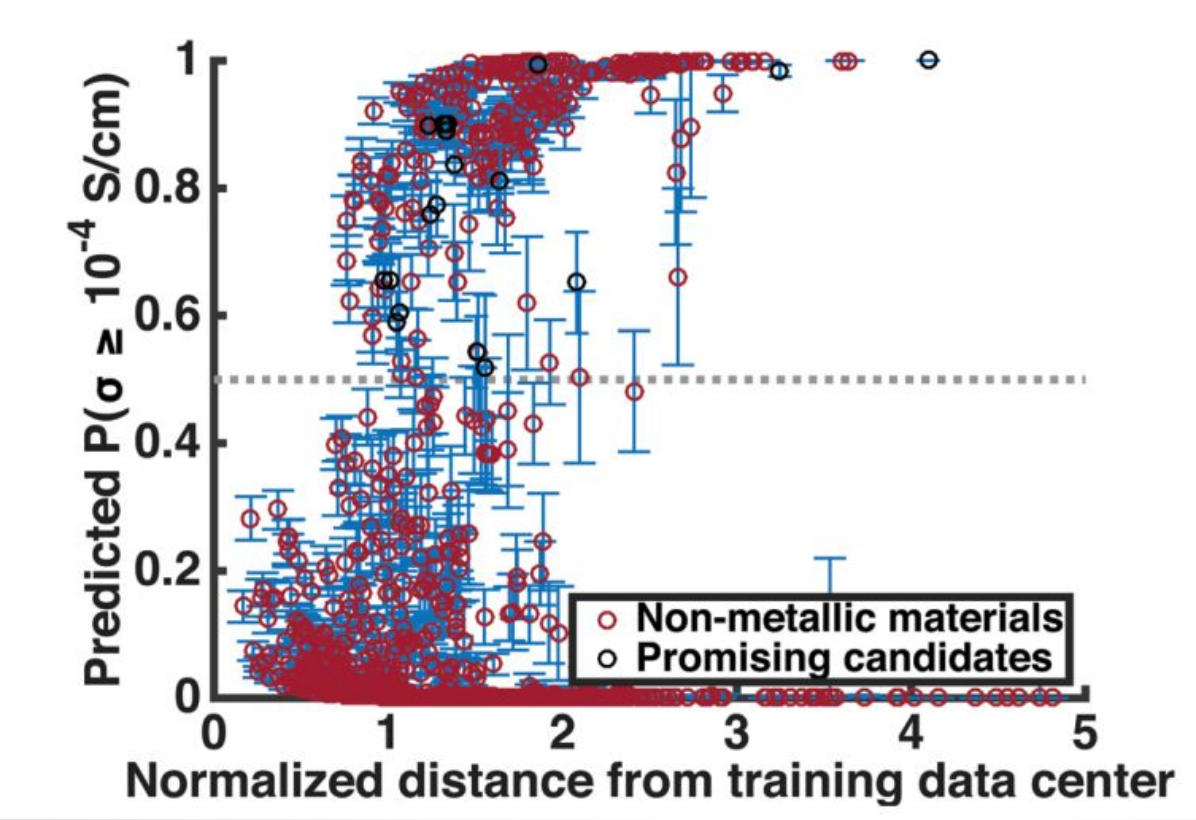

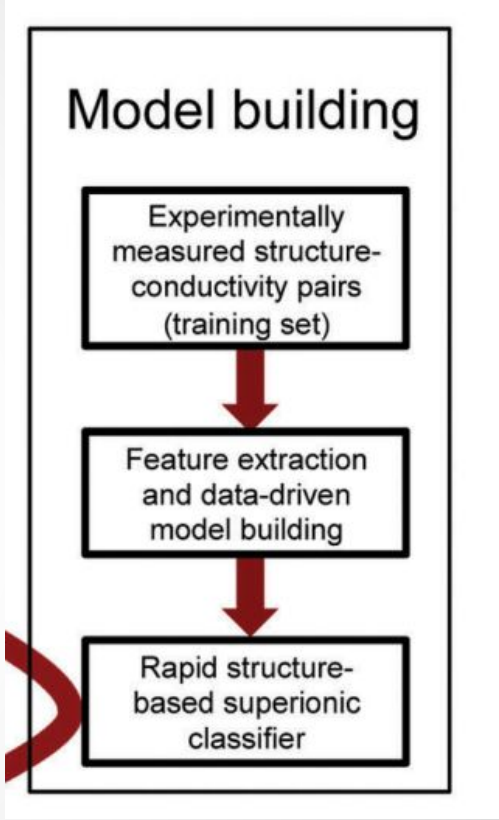

Sendek, Austin D., et al. "Holistic computational structure screening of more than 12000 candidates for solid lithium-ion conductor materials." *Energy & Environmental Science* 10.1 (2017): 306-320.

Development of code SIMAN for Automation of DFT calculations

- **SIMAN** package, on github https://github.com/dimonaks/siman (~30 000 lines of code)
  - generation of input files for VASP (DFT) or other codes
  - batch submission of hundreds of jobs and workflows
  - extraction and advanced analysis of output results
  - 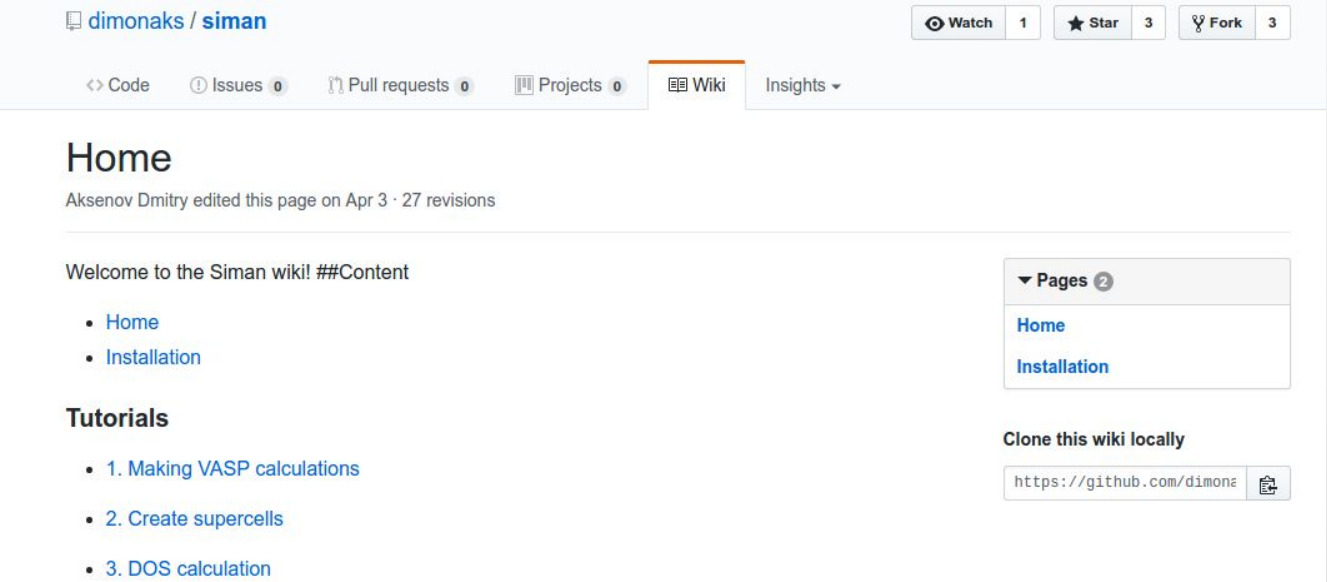

Optimize volume using Siman at two e-cut

```
new = InputSet()
new.read_incar('INCAR')
```

The set can be added to the predefined persistent dictionary by

```
sets['S400'] = new
```

```
read_vasp_sets([('S600','S400', {'ENCUT':600})])
```

```
add('Li2bcc', ['S400', 'S600'], 1, run = 1,
    calc_method = 'uniform_scale')
```

Results of optimization

```
res('Li2bcc', ['S400', 'S600'],
    [1,2,3,4,5,6,7,100], analys_type = 'fit_a')
```

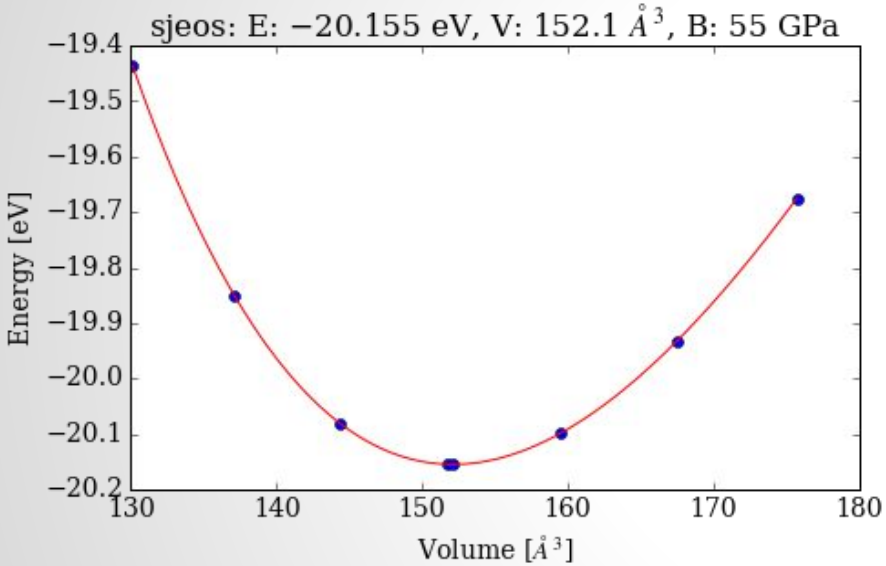

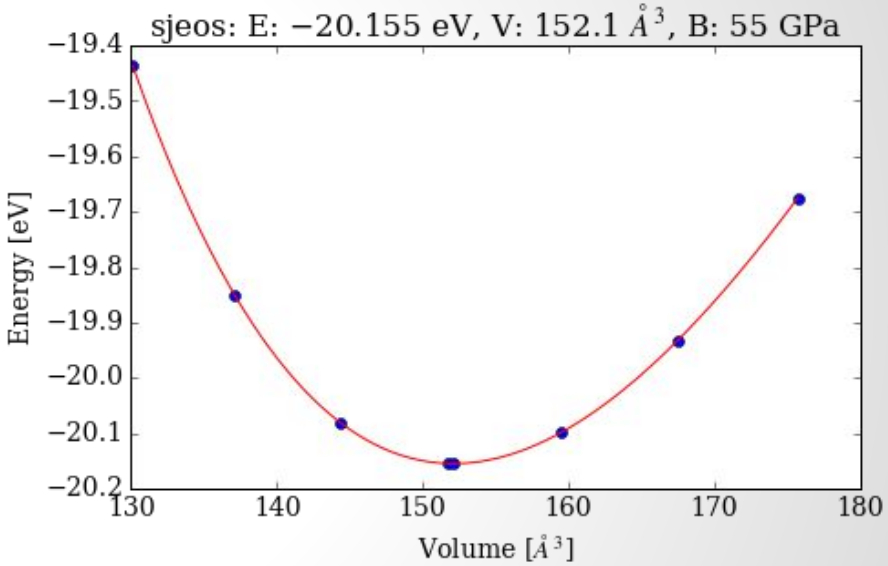

- In the same manner, each step required in calculations is automated
- Very useful when you have several structures and elements to study

Outline

1. Motivation to study energy materials and introduction into battery components

2. Modeling of solid electrodes

3. Modeling of electrolytes and interfaces

4. High-throughput modeling

5. Few examples from our experience: OH defects in $LiFePO_4$, antisite defects in layered oxides, migration barriers in cathodes

Our method for electronic structure calculation

- DFT + U (VASP code)
- U = 6.2 (Ni), 3.4 (Co) , 4.0 (Fe), 3.1 (V) eV
- PAW PBE potentials
- Spin polarized ferromagnetic
- Dipole correction for slab
- Energy cut-off 400 eV
- kpoint density 0.03 $Å^{-1}$
- Forces less than 0.05 eV/Å

Case study: point defects in cathodes

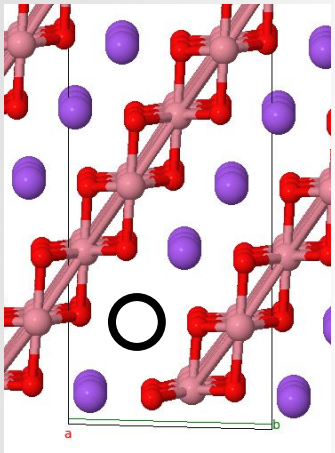

Vacancies

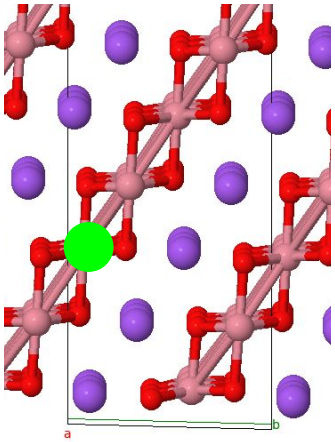

Dopants

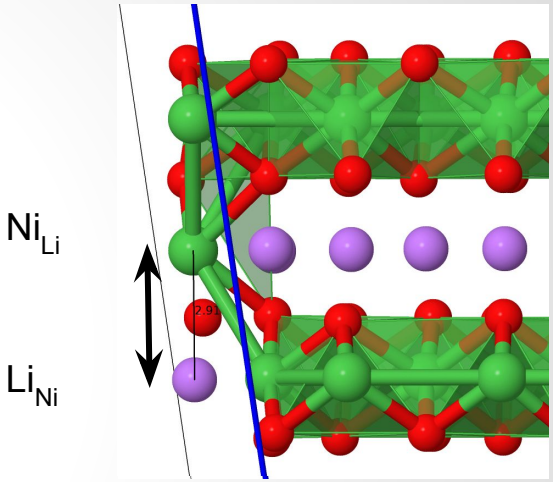

Anti-structure defect

- Point defects have influence on ionic and electronic conductivity and its mechanism
- Play key role in degradation of cathode materials

Unusual point defects in $LiFePO_4$

Formula	name	a	b	c
$LiFePO_4$	triphylite	4.70	6.00	10.33

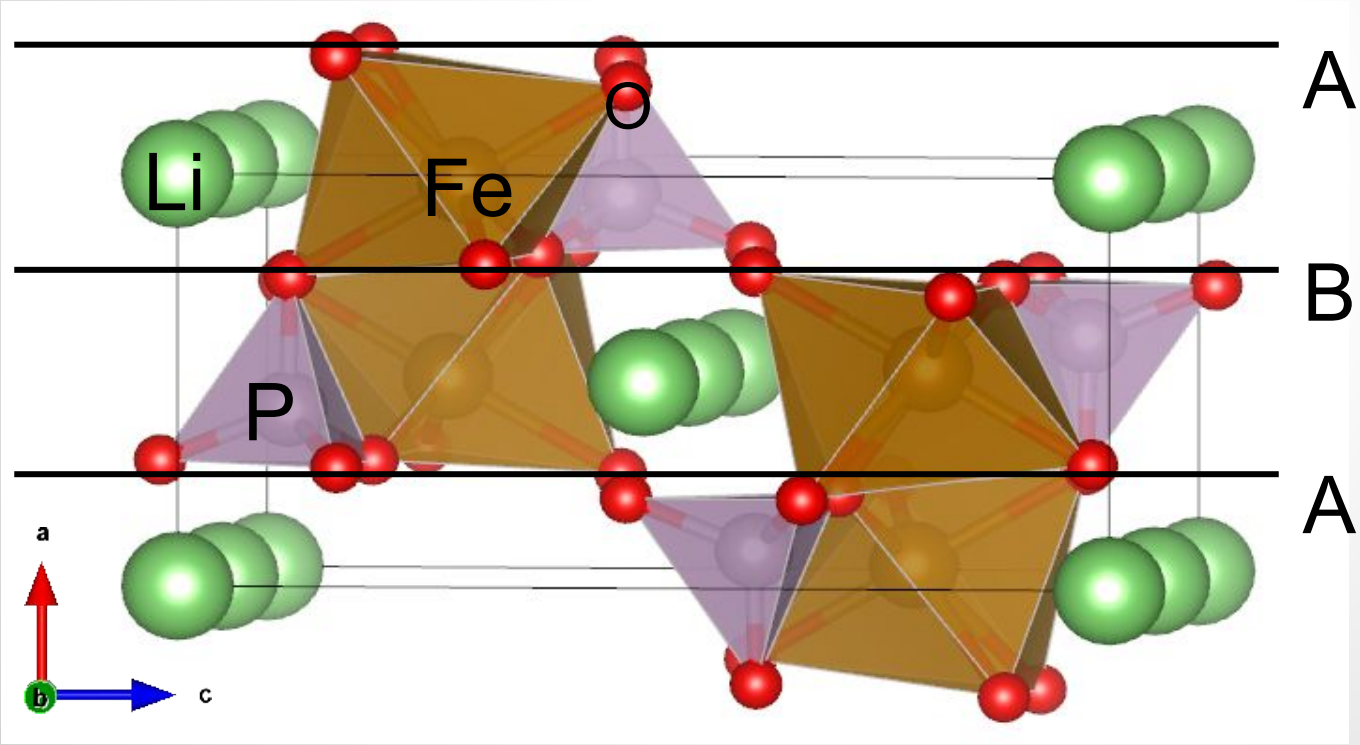

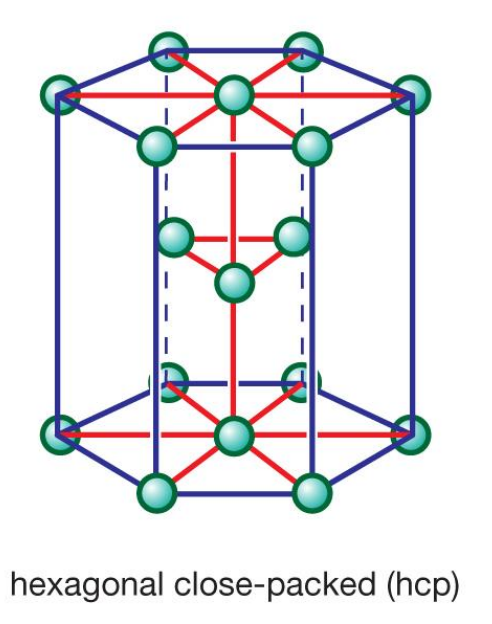

Experimentally observed compositions obtained with hydrothermal synthesis at Skoltech and MSU

$Li_{0.93}Fe_{1.07}P_{0.84}$
$Li_{0.95}Fe_{1.05}P_{0.87}$
$Li_{0.98}Fe_{1.02}P_{0.88}$

Up to 16% of P vacancies!

Is it possible in $LiFePO_4$?

Sumanov, V D., **D.A. Aksyonov**, O.A. Drozhzhin, et al. // *Chemistry of Materials* 31, no. 14 (2019): 5035-5046.

Li-Fe-P-O phase diagram, $\mu(O_2) = -12.4$ eV

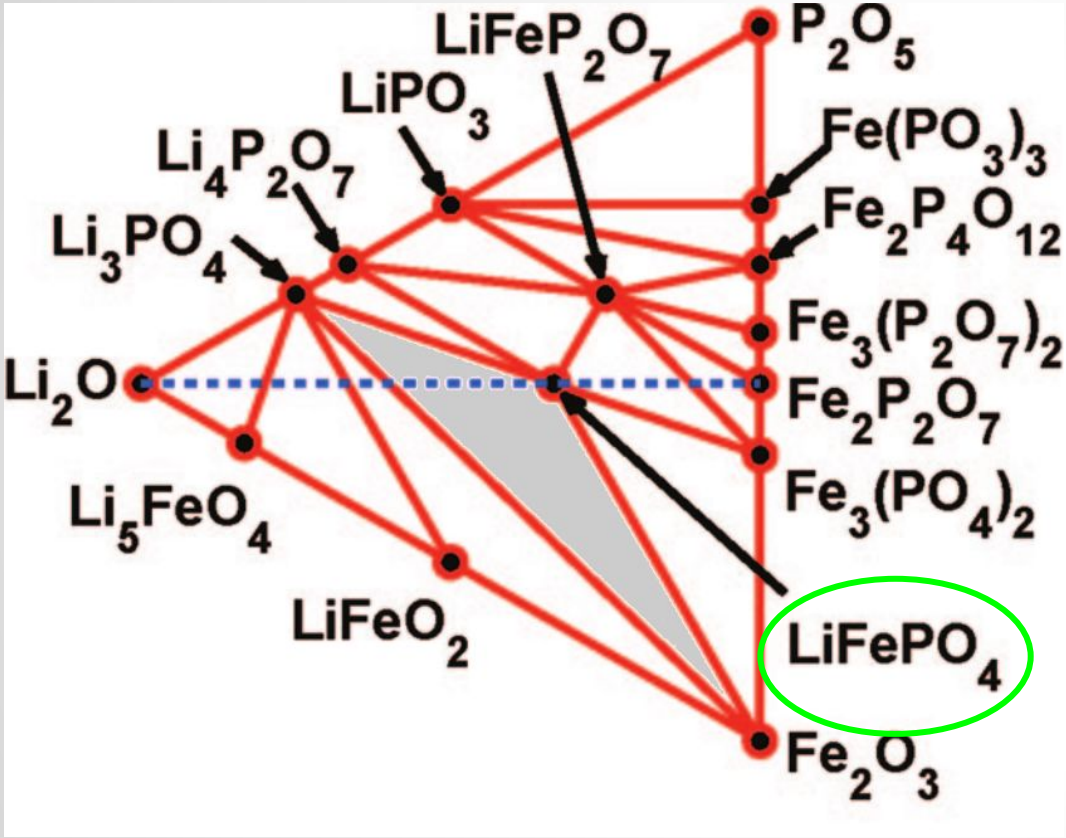

Li_3PO4 - $LiFePO_4$ - Fe_2O_3 region is stable for $\mu(O_2)$ from –13.0 eV to –11.5 eV

$\mu(Fe) = 1/2\ [\mu(Fe_2O_3) - 3/2\ \mu(O_2)]$

$\mu(Li) = 1/2\ [\mu(Li_3PO_4) - \mu(LiFePO_4) + \mu(Fe)\ ]$

$\mu(P) = 1/2\ [3\ \mu(LiFePO_4) - \mu(Li_3PO_4) - 3\ \mu(Fe) - 4\ \mu(O_2)]$,

1. Ong, S.P., Wang, L., Kang, B. and Ceder, G. Li–Fe–P–O2 Phase Diagram from First Principles Calculations. Chemistry of Materials. 20, 5 (Mar. 2008), 1798–1807.

Formation energy of P vacancies

$$dE = [E(LiFeP_{1-x}Vac_xO_4) - E(LiFePO_4) + x\mu(P)]/x$$

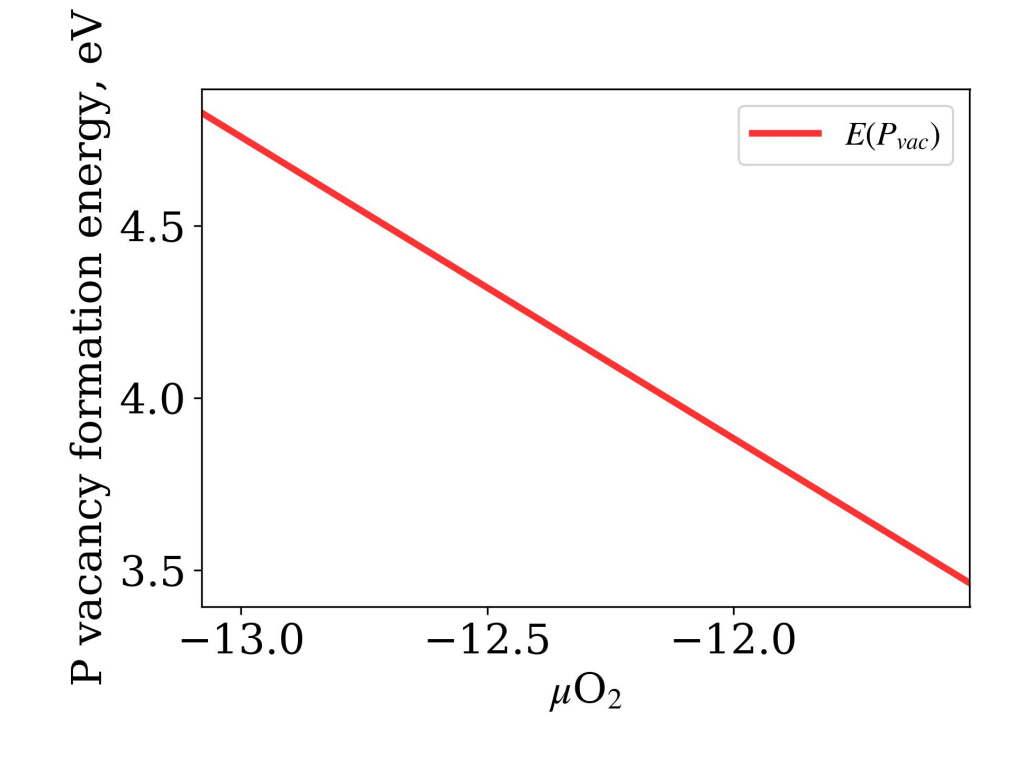

$C_{vac} = \exp(-3.5/kT) \sim 10^{-36}$ at T = 473 K - no vacancies are possible

How the P vacancy energy can be reduced?

In metals, hydrogen is trapped in vacancies

E.g. in tungsten up to 12 H go into vacancy

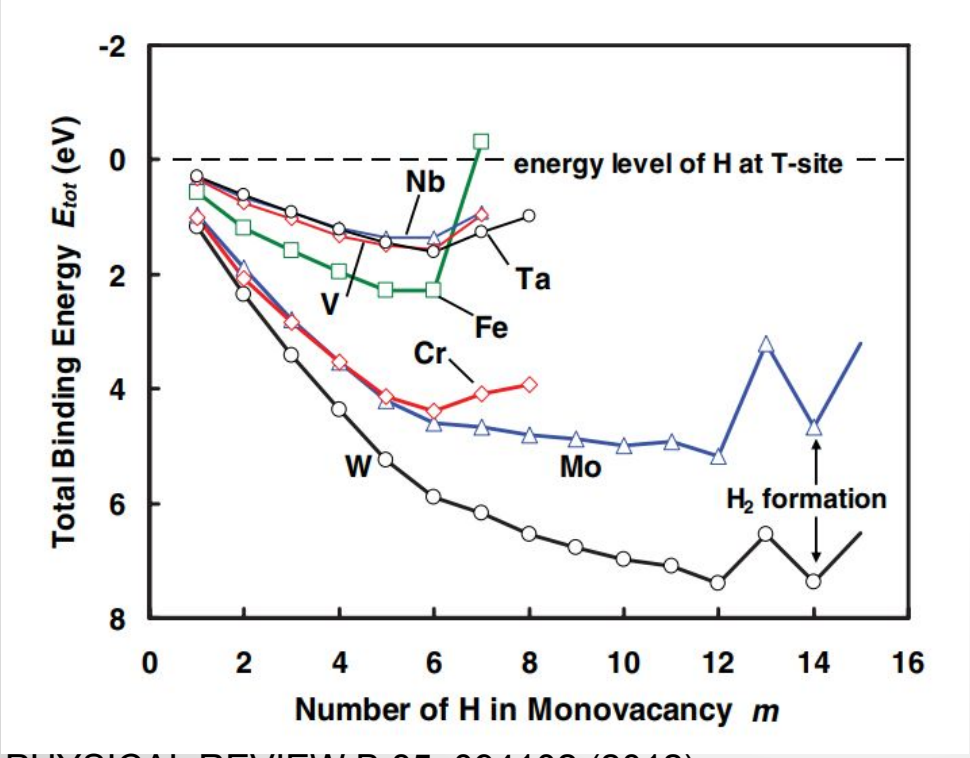

PHYSICAL REVIEW B 85, 094102 (2012)

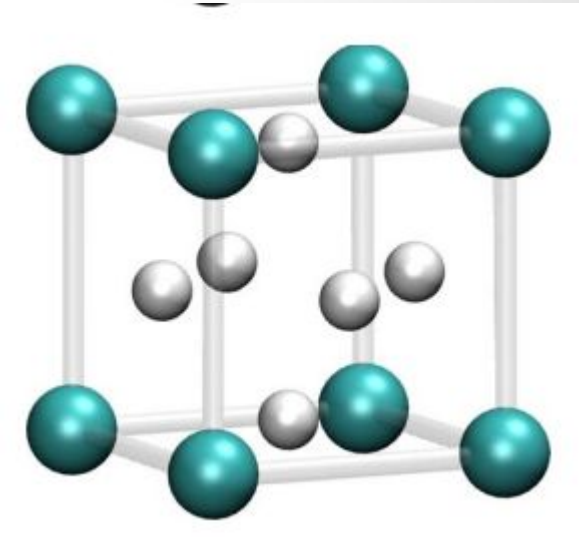

8 H in vacancy in tungsten

PHYSICAL REVIEW B 82, 094102 2010

What if 4 hydrogens substitute one P?

$$E_{sub} = [E(LiFeP_{1-x}Vac_xH_{4x}O_4) - E(LiFePO_4) + x\mu(P) - 4\mu(H)]/4x$$

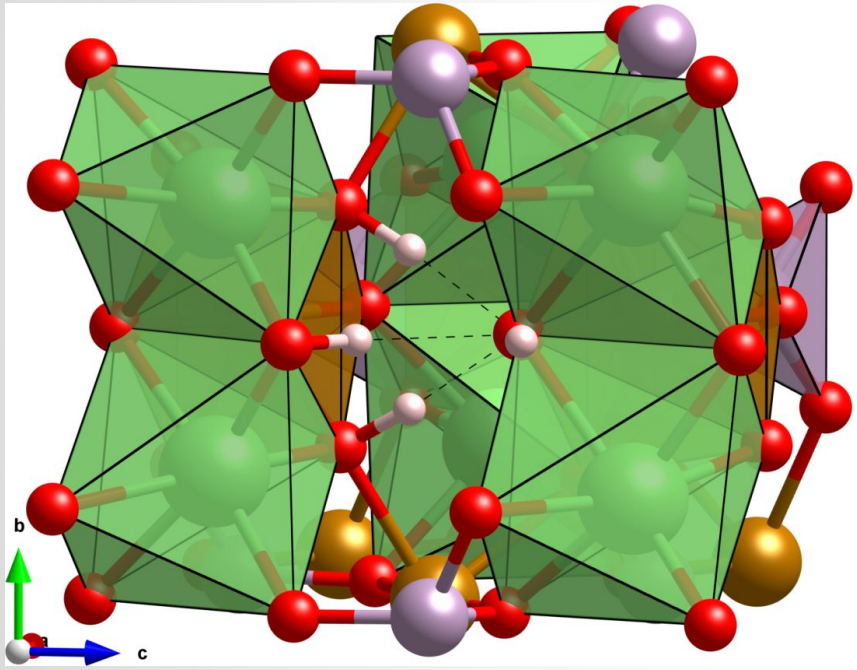

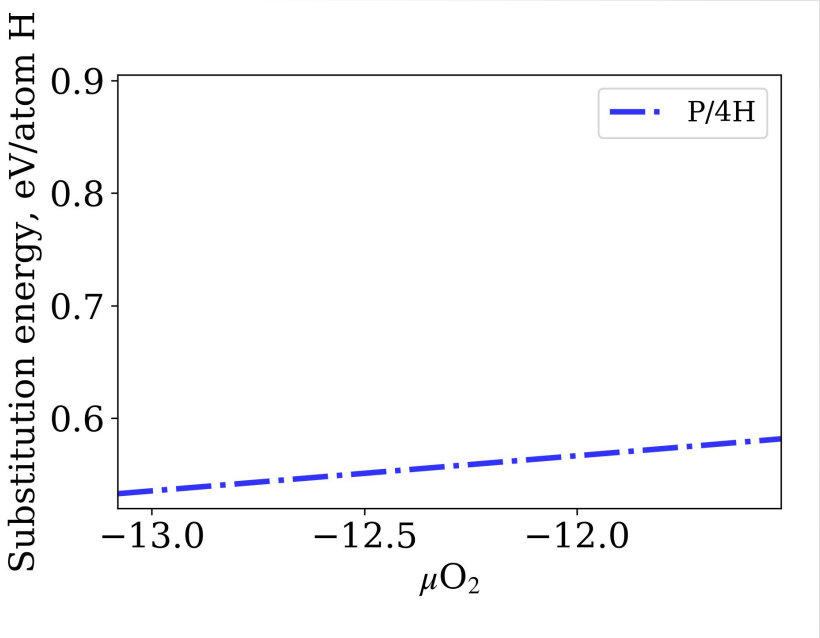

Hydrogen stabilize P vacancy reducing it's formation energy from 4.8 eV to 2.1 eV

What about other substitutions?

1 H in octa

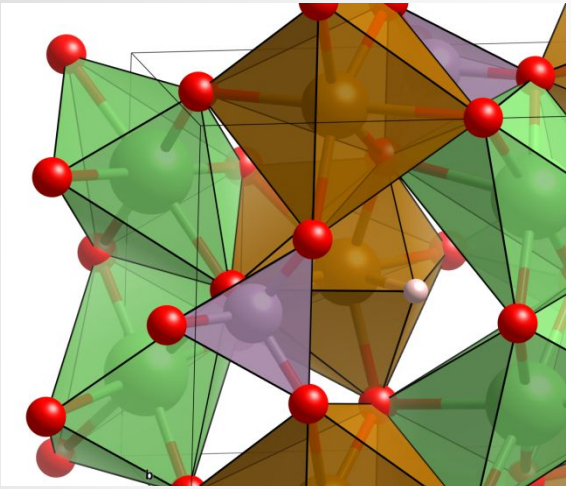

H/Li sub

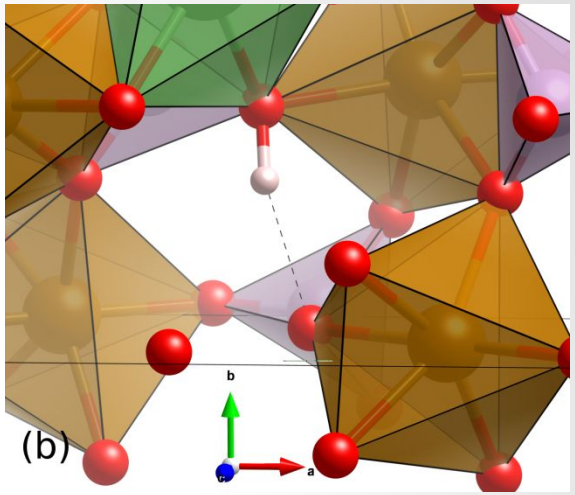

2H/Fe sub

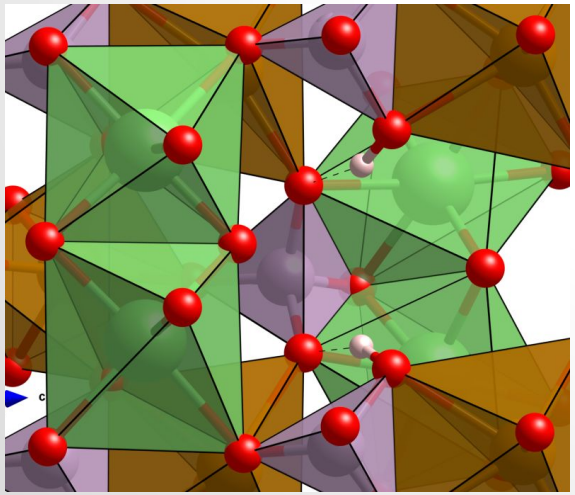

Dependence from O_2 chemical potential

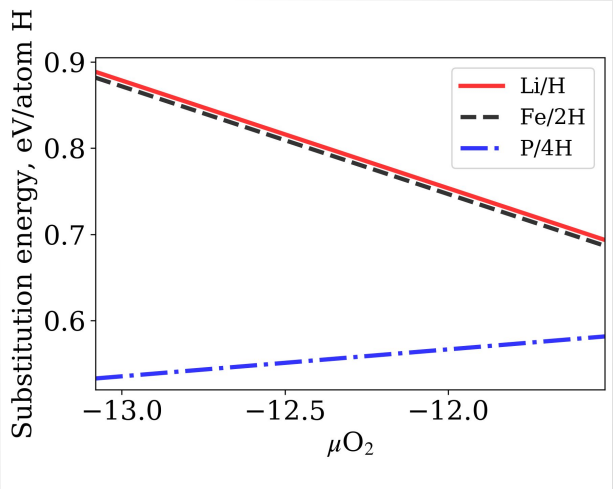

Experimental confirmation of 4H defect

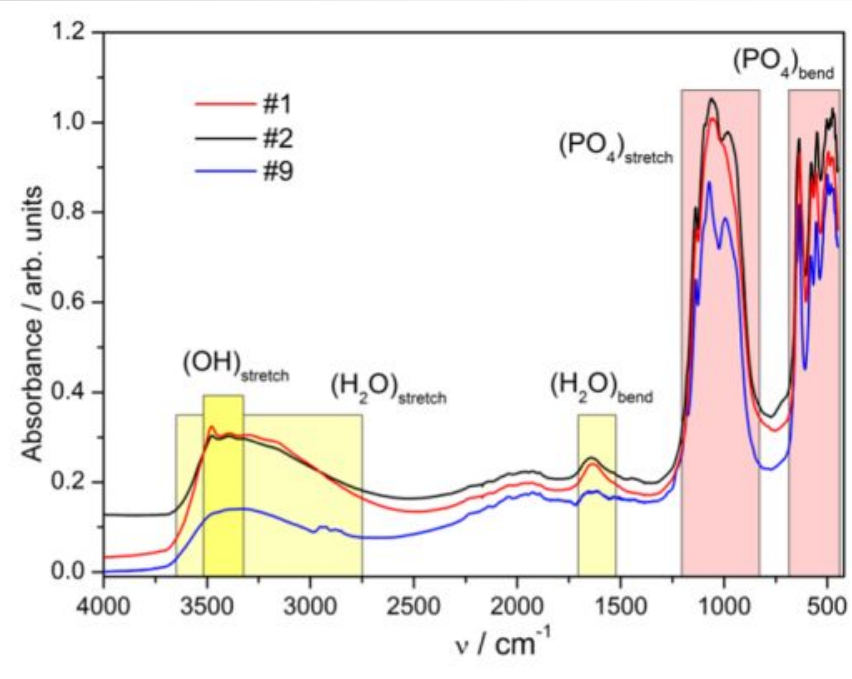

- After theoretical prediction the existence of 4H defects was confirmed experimentally at our center using both Mossbauer and Infrared spectroscopy.

- However, the exact atomic structure of defect is known only from DFT calculations

Sumanov, Vasily D., Dmitry A. Aksyonov, Oleg A. Drozhzhin, Igor Presniakov, Alexey V. Sobolev, Iana Glazkova, Alexander A. Tsirlin et al. ""Hydrotriphylites" Li1–x Fe1+ x (PO4) 1–y (OH) 4 y as Cathode Materials for Li-ion Batteries." *Chemistry of Materials* 31, no. 14 (2019): 5035-5046.

In mineral world hydrogarnet defect in Mg_2SiO_4 is known for a long time

Phys Chem Minerals (1983) 9:57–60

PHYSICS AND CHEMISTRY OF MINERALS

A Model of the OH Positions in Olivine, Derived from Infrared-Spectroscopic Investigations

A. Beran[1] and A. Putnis[2]

[1] Institut für Mineralogie und Kristallographie der Universität Wien, Dr. Karl Lueger-Ring 1, 1010 Vienna, Austria

[2] Department of Earth Sciences, University of Cambridge, Downing Street, Cambridge CB2 3EQ, England

- First experimental evidence of hydrogarnet type defect in olivine was obtained by Beran and Putnis in **1983** (though P/3H)
- DFT calculations for P/4H in Mg_2SiO_4 was done in **2000** by Brodholt and Refson

JOURNAL OF GEOPHYSICAL RESEARCH, VOL. 105, NO. B8, PAGES 18,977–18,982, AUGUST 10, 2000

An ab initio study of hydrogen in forsterite and a possible mechanism for hydrolytic weakening

John P. Brodholt

Department of Earth and Planetary Sciences, University College London, London

Keith Refson

Department of Earth Science, University of Oxford, Oxford, England

Abstract. Even small amounts of water can profoundly effect the physical properties of minerals. In olivine <1 H in every 1000 unit cells acts to increase creep rates of dunite by ~ 2 orders of magnitude. Although the mechanism for this is not known, it is not unreasonable to suggest that it is in some way related to an increase in the point defect population. In order to understand this better we have performed ab initio pseudopotential calculations within the generalized gradient approximation on protonic defects in Mg_2SiO_4 forsterite. Three mechanisms for incorporating protons are considered: (1) interstitial, (2) binding at cation vacancies, and (3) binding at silicon vacancies. Assuming the existence of both Si

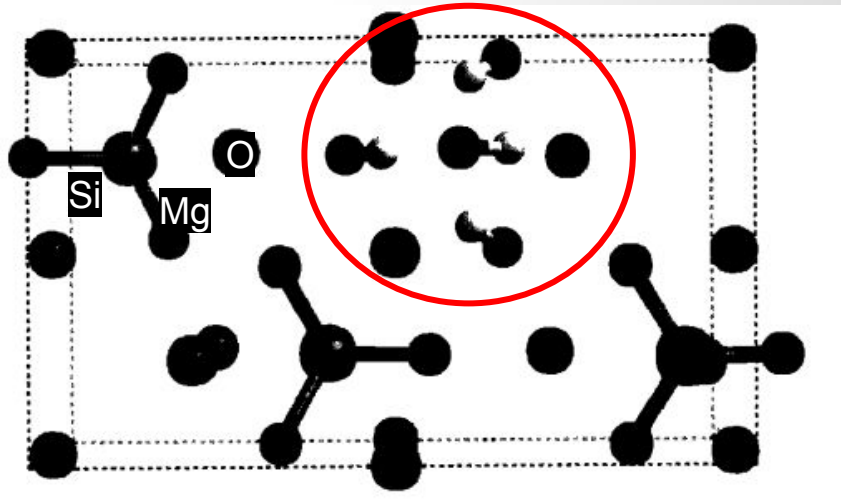

Outline

1. Motivation to study energy materials and introduction into battery components

2. Modeling of solid electrodes

3. Modeling of electrolytes and interfaces

4. High-throughput modeling

5. Few examples from our experience: OH defects in $LiFePO_4$, antisite defects in layered oxides, migration barriers in cathodes

Morphology and surface structure of cathode particles is highly important!

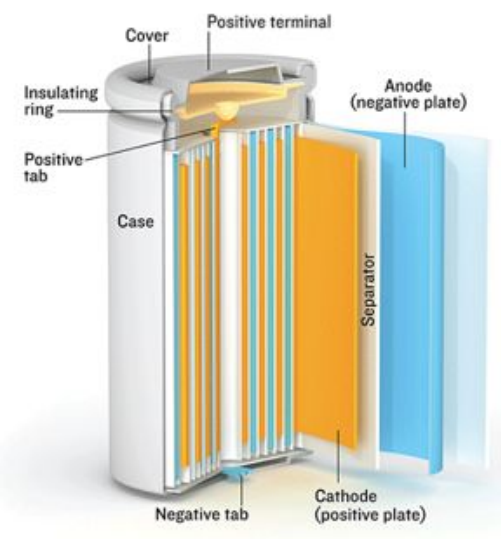

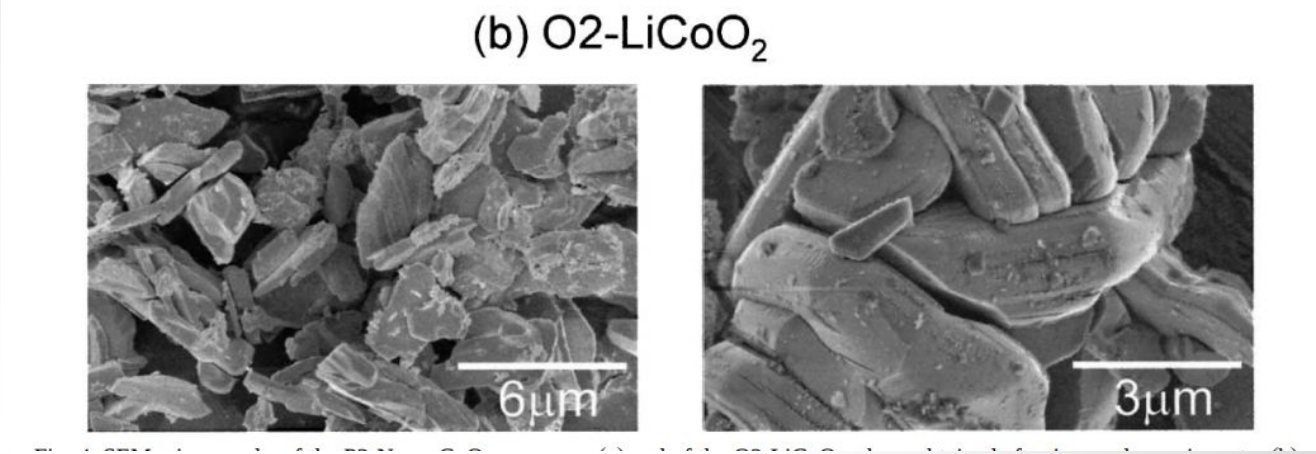

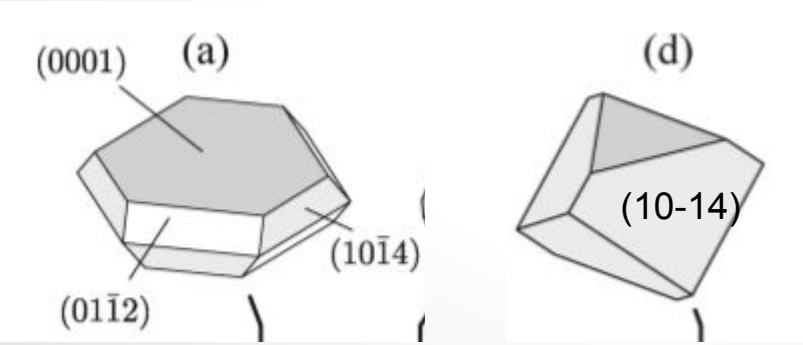

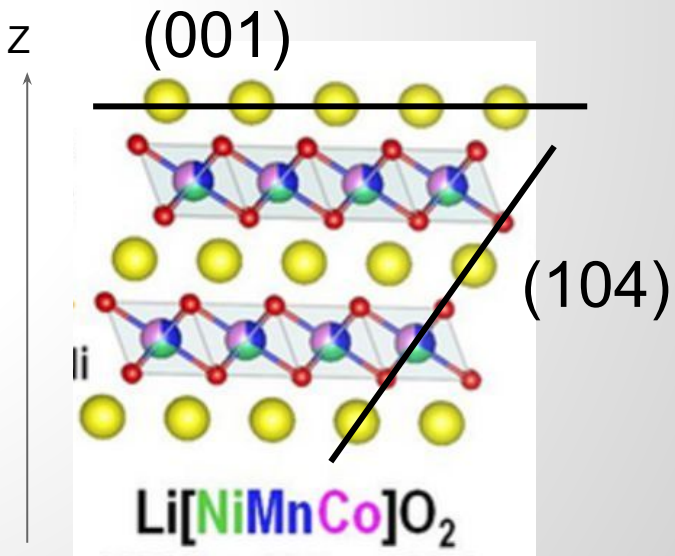

Carlier2001 Kramer2009

What happens on the surface?

Rocksalt-type surface reconstruction

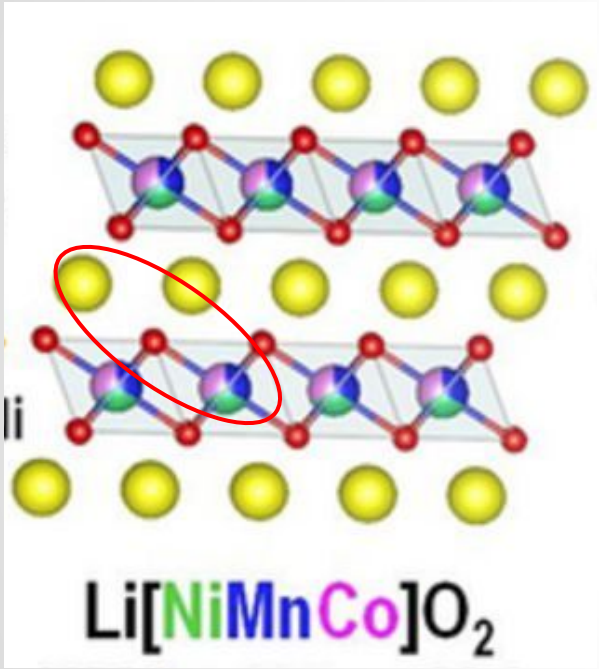

TEM of (104)

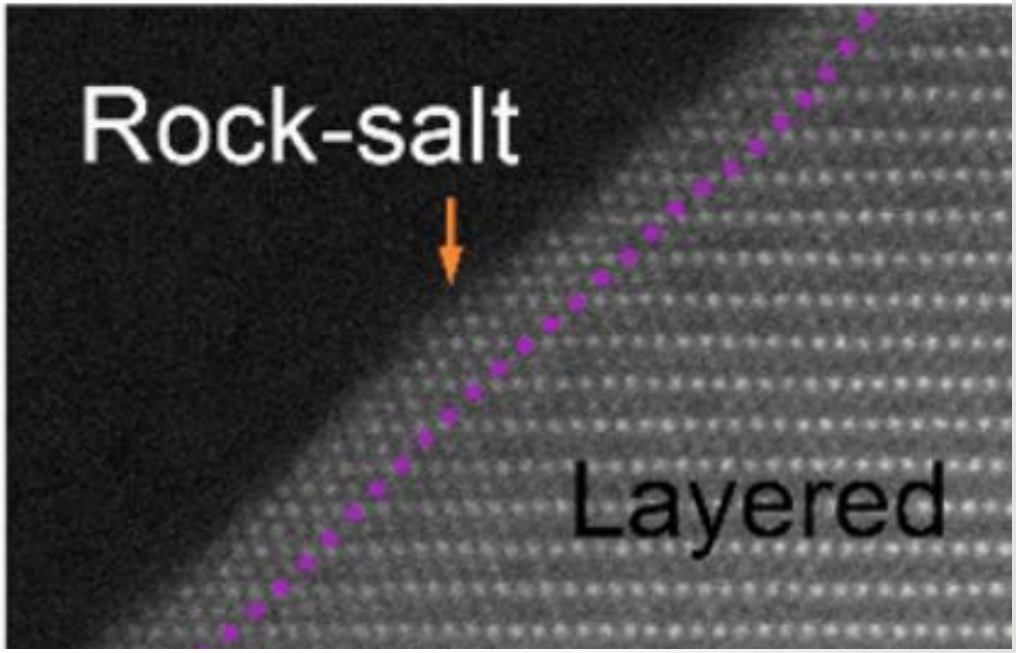

(104)hex -> (002)cubic

Zhang2018

Main question

Is surface reconstruction based on antisite pairs kinetically controlled or any thermodynamic driving force exists?

↓

Make DFT+U atomic simulation neglecting the influence of electrolyte.

Formation energy of antisites

Very important type of defects in layered oxides, up to 10% in $LiNiO_2$, but much smaller in $LiCoO_2$

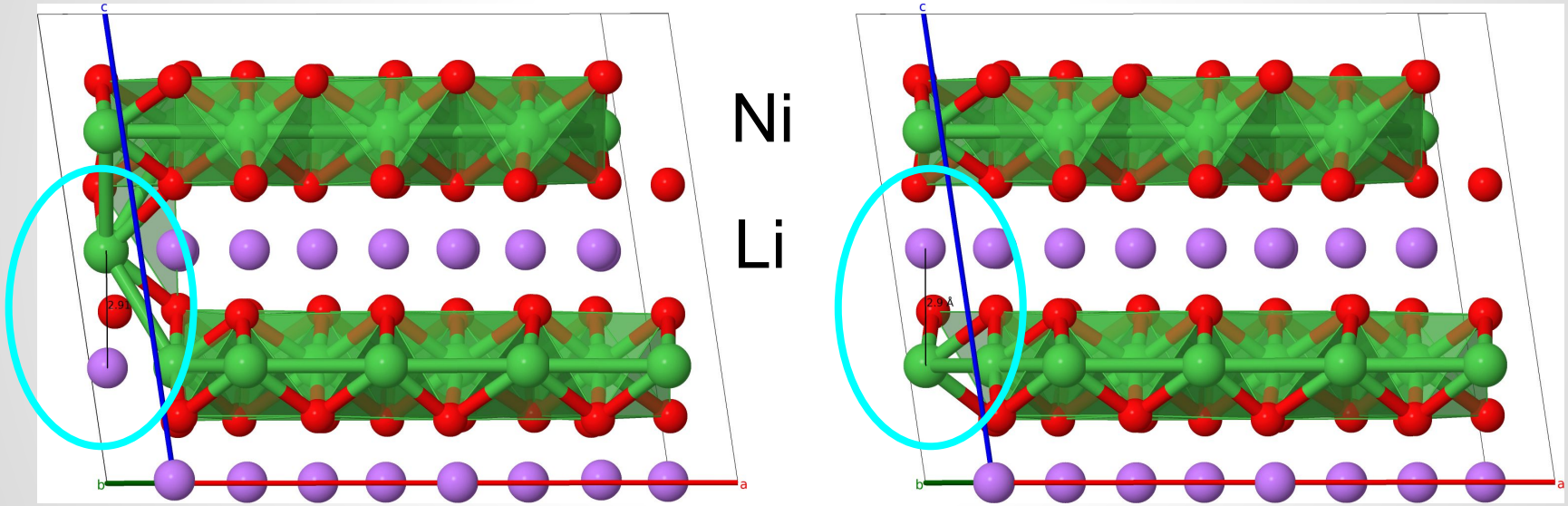

dE_{AS} = E(supercell with antisite) - E (ideal supercell)

Siman code: creating antisite defects

```
In [12]: NCO = smart_structure_read('geo/POSCAR_NaCoO2')
         create_antisite_defect(NCO, 'Na', 'Co', max_sep = 6, iatom = 1)
```

```
-- List of antisites:

+-------+-----------------+-------+-------+-----------------+
|   No. | Antisite type   |   at1 |   at2 |   Separation, A |
|-------+-----------------+-------+-------+-----------------|
|     0 | (0, 32)         |     2 |    35 |           3.091 |
|     1 | (0, 32)         |     2 |    34 |           4.247 |
|     2 | (0, 32)         |     2 |    33 |           5.15  |
+-------+-----------------+-------+-------+-----------------+
```

Antisite pairs formation energies

Phase	space group	AS energy
$LiNiO_2$	R-3m	− 0.8 eV
$LiCoO_2$	R-3m	1.9 eV
$NaNiO_2$	C2/m	2.1 eV
$NaCoO_2$	R-3m	2.9 eV

Negative antisite formation energy for $LiNiO_2$!

May be the problem with $LiNiO_2$ space group?

- **$LiNiO_2$** is often reported in **R-3m** group, where all Ni-O bonds are fixed to 1.99 Å.

- However Jahn-Teller (**JT**) distortion and charge ordering of Ni^{3+} to Ni^{2+} and Ni^{4+} are possible with the reduction of energy

$LiNiO_2$ in P2/c with charge order is most stable

PHYSICAL REVIEW B **84**, 085108 (2011)

Charge disproportionation and Jahn-Teller distortion in $LiNiO_2$ and $NaNiO_2$: A density functional theory study

Hungru Chen,* Colin L. Freeman, and John H. Harding
Department of Materials Science and Engineering, University of Sheffield, S1 3JD, United Kingdom
(Received 24 March 2011; revised manuscript received 12 July 2011; published 19 August 2011)

Density functional theory calculations have been performed on three potential ground-state configurations of $LiNiO_2$ and $NaNiO_2$. These calculations show that, whereas $NaNiO_2$ shows the expected cooperative Jahn–Teller distortion (and therefore a crystal structure with $C2/m$ symmetry), $LiNiO_2$ shows at least two possible crystal structures very close in energy (within 3 meV/formula unit): $P2_1/c$ and $P2/c$. Moreover, one of them ($P2/c$) shows charge disproportionation of the (expected) Ni^{3+} cations into Ni^{2+} and Ni^{4+}. We discuss the implications of this complex ground state for the interpretation of the available electron and neutron structure data, its electronic and comple

DOI: 10.11(

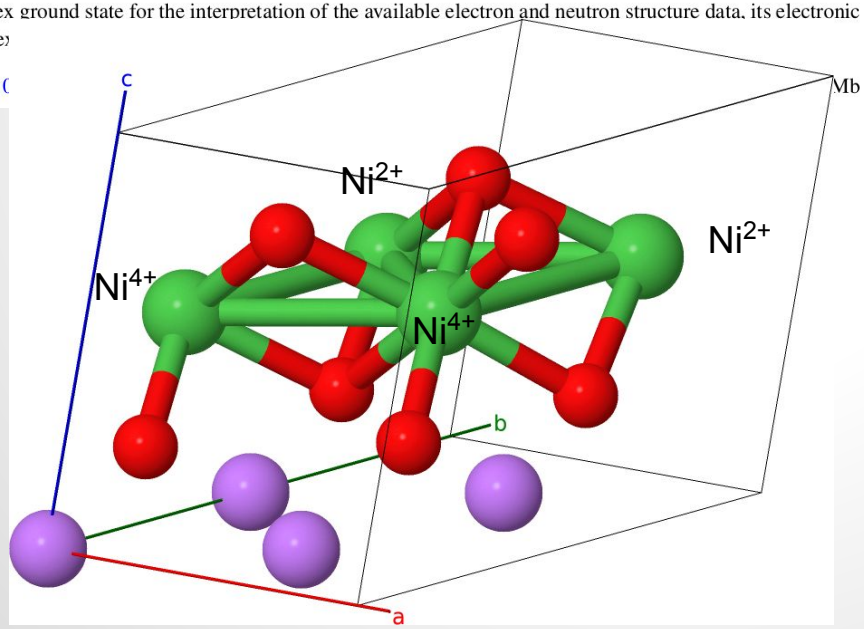

- Charge-disproportionation of Ni^{3+} to Ni^{2+} and Ni^{4+}
- According to our results the total energy reduced by **15 meV/atom**
- 1.5 eV for 100-atom cell!

Antisite pairs formation energies

Phase	space group	AS energy	NN, sep, A
$LiNiO_2$	P2/c	0.73 eV (0.75 [1])	1nn, 2.86 A
$LiCoO_2$	R-3m	1.9 eV	1nn, 2.82 A
$NaNiO_2$	C2/m	2.1 eV	2nn, 4.17 A
$NaCoO_2$	R-3m	2.9 eV	2nn, 4.22 A

Chen, Hungru, James A. Dawson, and John H. Harding. "Effects of cationic substitution on structural defects in layered cathode materials LiNiO 2." *Journal of Materials Chemistry A*2, no. 21 (2014): 7988-7996.

Surface energy calculations

For Polar

non-stoichiometric

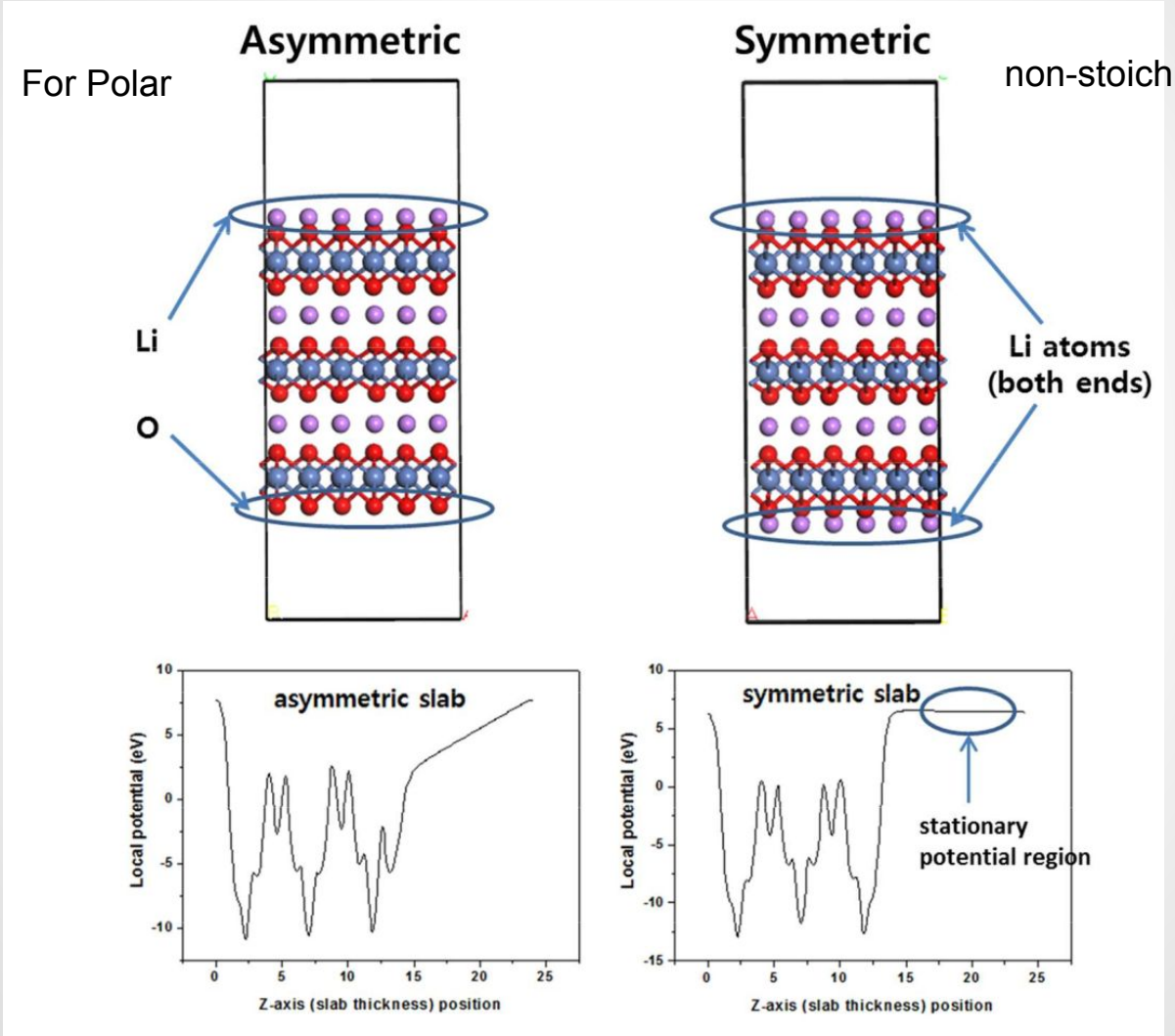

Cho E., Seo S. W., Min K. ACS applied materials & interfaces. – 2017. – Т. 9. – №. 38. – С. 33257-33266./SI

Surface energies

$$\gamma = \frac{1}{2 \cdot A}\left[E_{\text{slab}} - N_{\text{Co}}\left(\varepsilon_{\text{b}} - \sum_i \Gamma_i \cdot \mu_i\right)\right]$$

ε_b is energy of bulk cell, Γ_i is excess of i atoms in the slab

Dependence on chemical potential !
phase diagram is required

Phase diagrams in chemical potential space

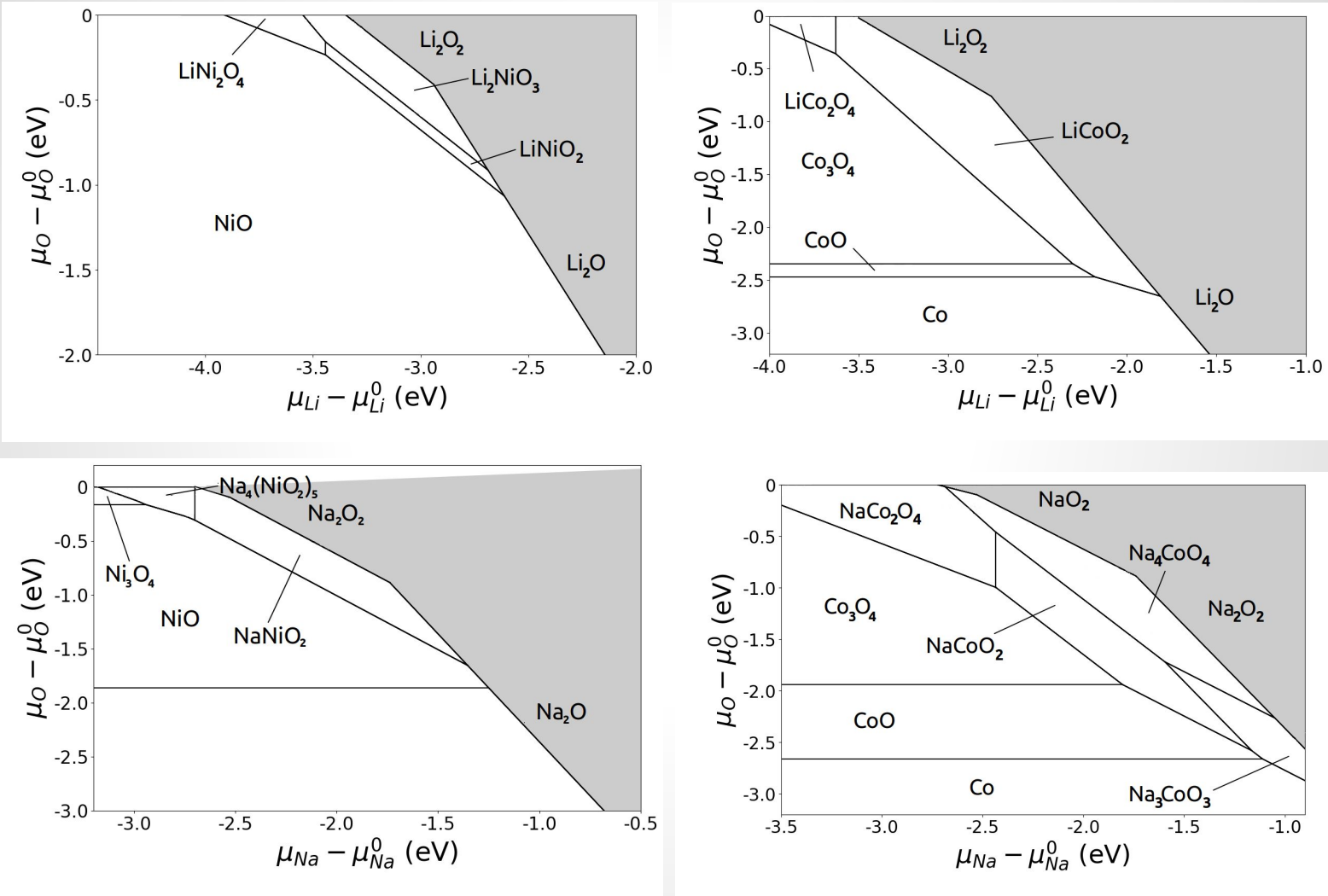

SIMAN: creating slabs with surfaces

```
st = create_surface2(sc, [0, 0, 1],
    cut_thickness = 10, min_vacuum_size = 10,
    symmetrize = 0, min_slab_size = 16)
```

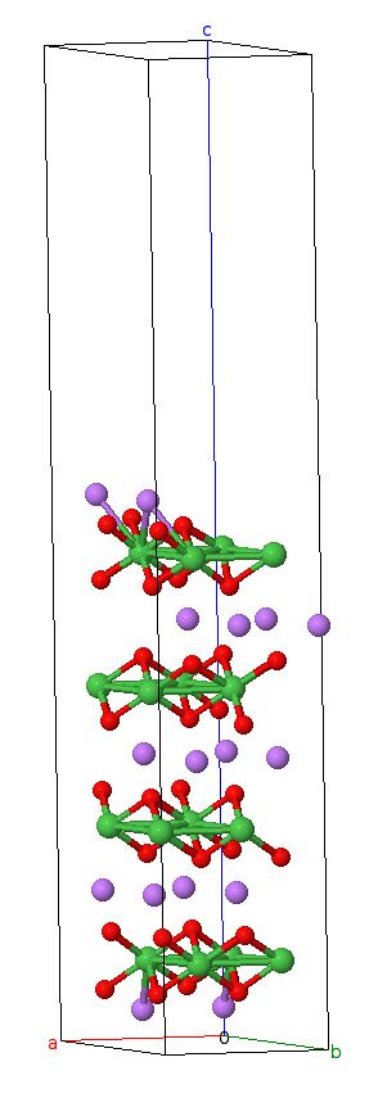

Surface energy (J/m^2) of considered oxides

Surface	$LiNiO_2$ (R-3m)	$LiCoO_2$ (R-3m)	$NaNiO_2$ (C2/m)	$NaCoO_2$ (R-3m)
(001) ½ ML	0.65	1.2	1.35	1.35
(104)/ (10-1)	0.55	1.1	0.35	0.87

Considered surfaces, example of $LiCoO_2$

R-3m: non-polar (104), (110), (100), polar : (012), (003), (101), (111)

C2/m: non-polar (104), (10-1), (100), (111), (10-2); polar - (003), (012), (110)

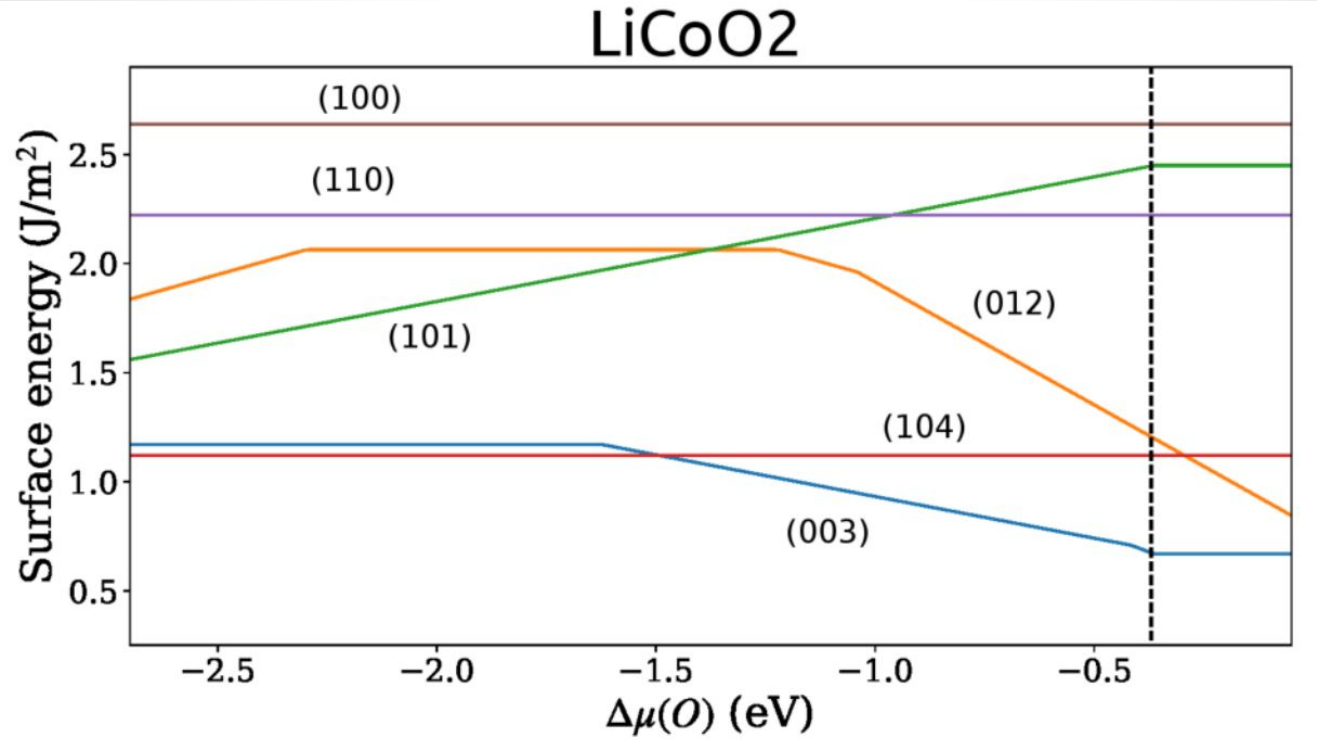

Dependence of surface energy on chemical potential

Wulff construction depending on chemical potential

$LiNiO_2$

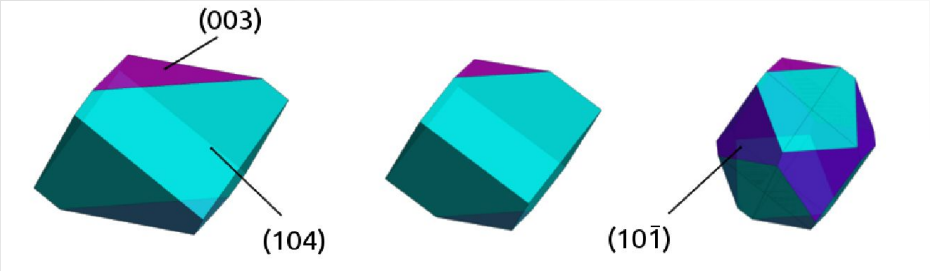

Wulff construction - minimizes the total surface energy for a given particle volume

$LiCoO_2$

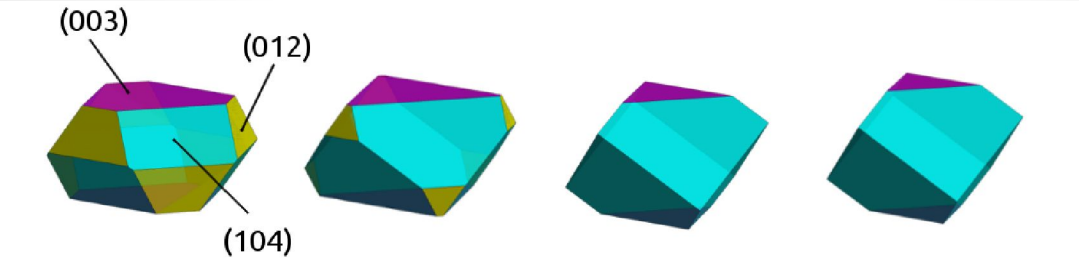

$NaNiO_2$

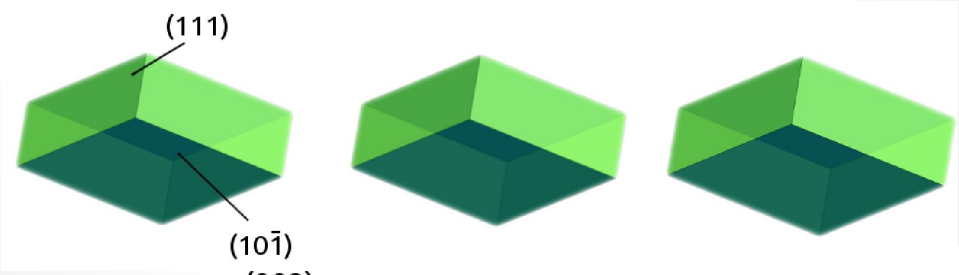

$NaCoO_2$

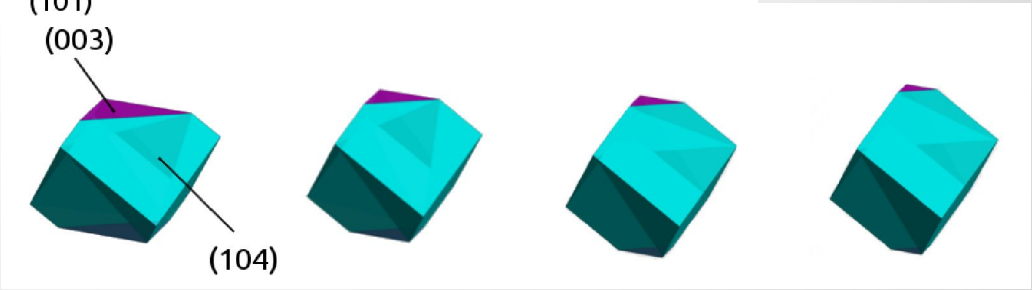

Surface antisites

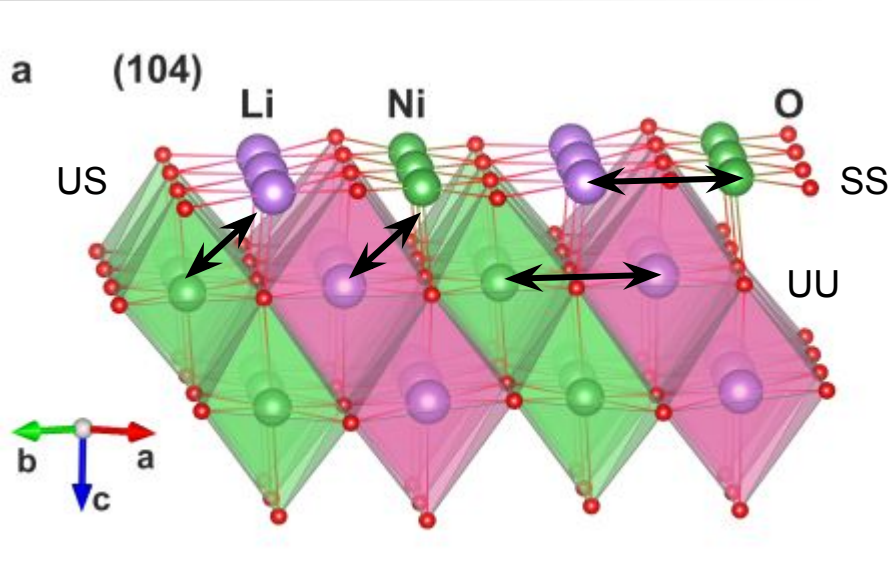

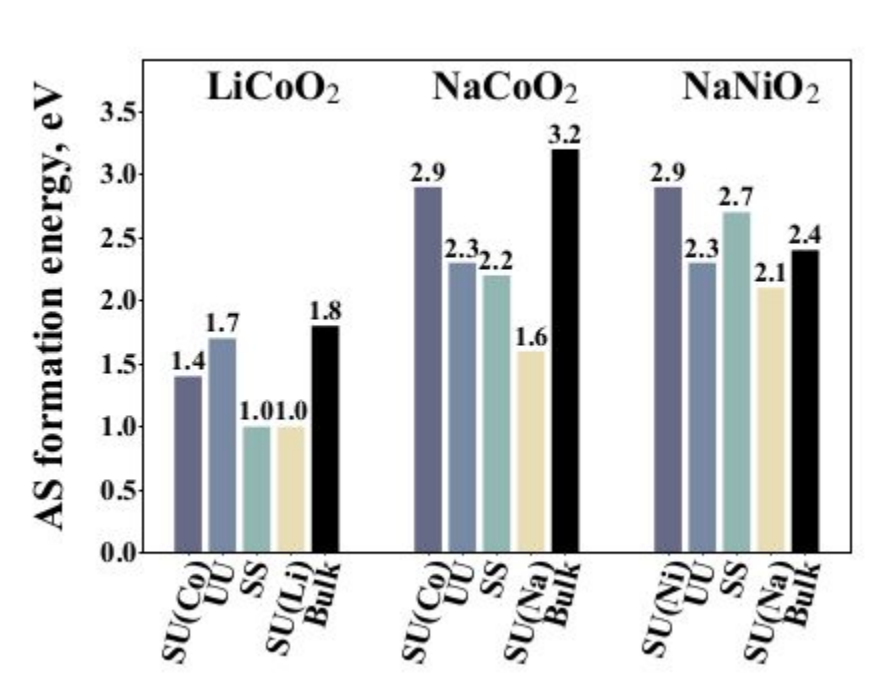

In Co-based oxides surface antisite pair is formed more easily, however the energy is still positive

- Influence of electrolyte?
- Kinetic control?
- Chemical composition change?

Outline

1. Motivation to study energy materials and introduction into battery components

2. Modeling of solid electrodes

3. Modeling of electrolytes and interfaces

4. High-throughput modeling

5. Few examples from our experience: OH defects in $LiFePO_4$, antisite defects in layered oxides, migration barriers in cathodes

Case study: migration barriers in cathodes

- **Ionic** and electronic conductivity of electrodes determines C-rate
- Ionic conductivity depends on diffusivity of cations
- Migration barrier should be less 0.3-0.4 eV

$$D = 1/2\Gamma d^2 \qquad \Gamma = \nu^* \exp\left(\frac{-\Delta E}{k_B T}\right)$$

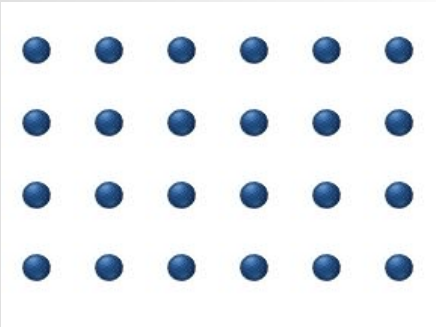

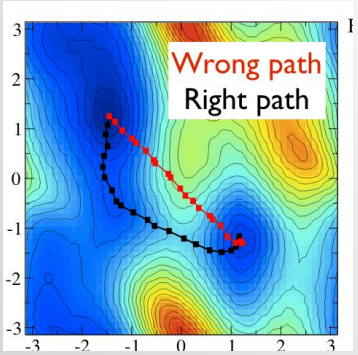

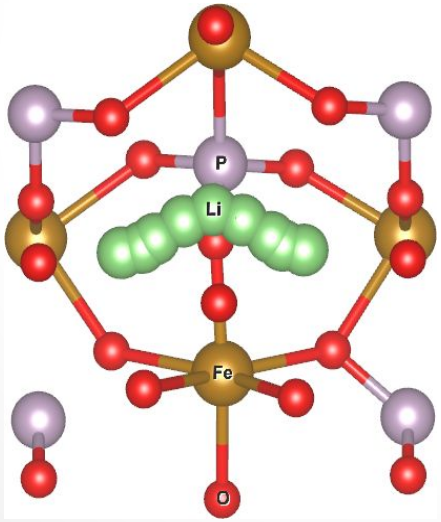

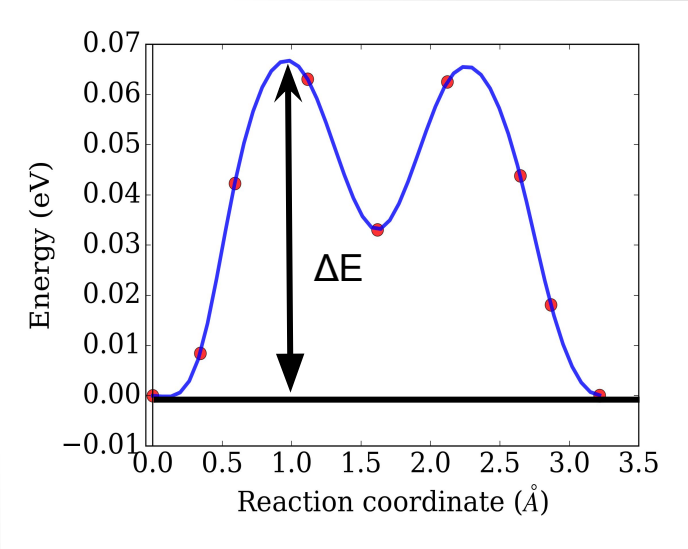

- Migration barrier can be calculated with Nudge elastic band method (NEB)

Migration of Na in $NaVP_2O_7$

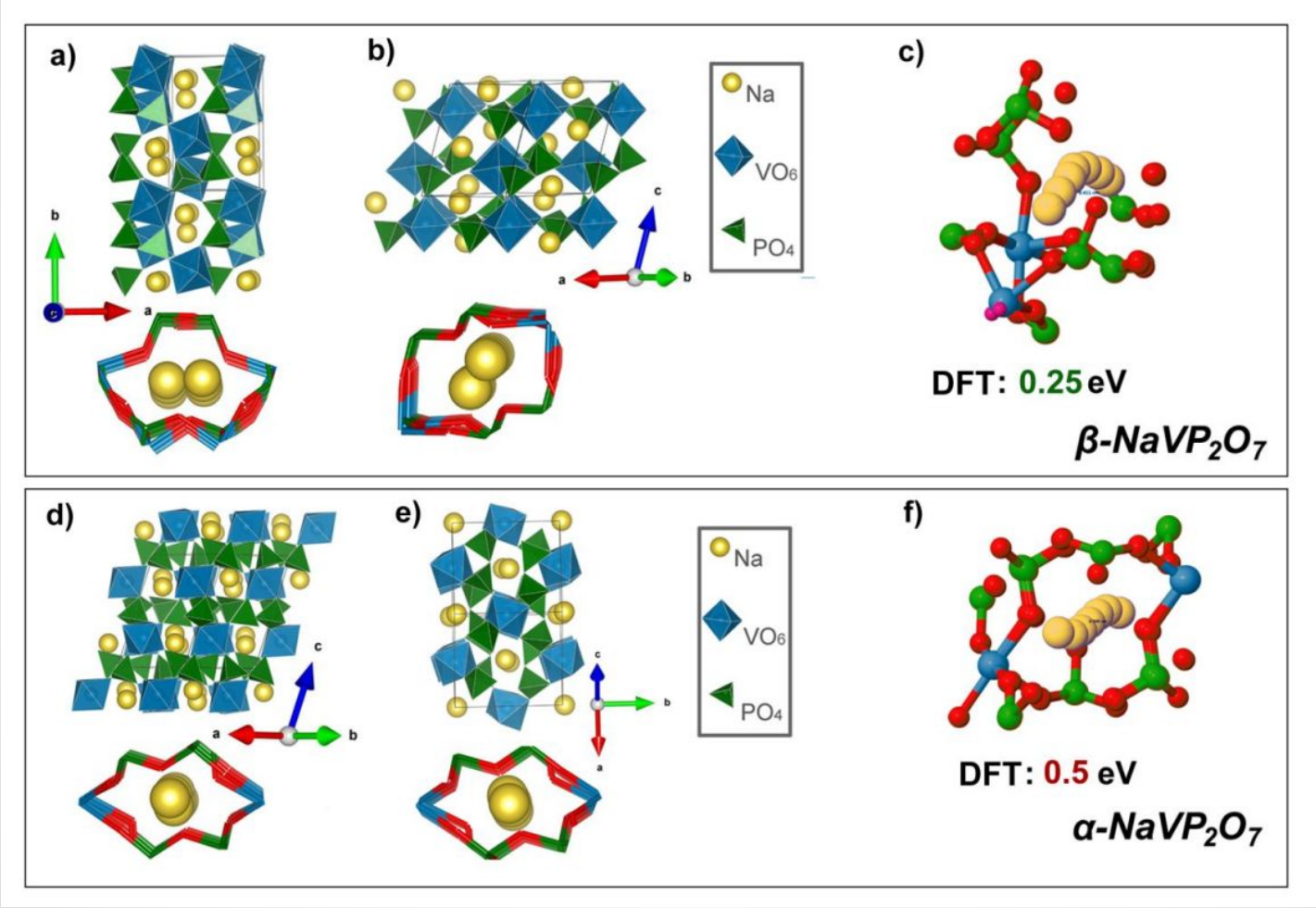

Drozhzhin, O.A., Tertov, I.V., Alekseeva, A.M., **Aksyonov, D.A.,** Stevenson, K.J., Abakumov, A.M. and Antipov, E.V., //. *Chemistry of Materials*, 2019

$KVPO_4F$ - new cathode materials developed by at MSU and Skoltech

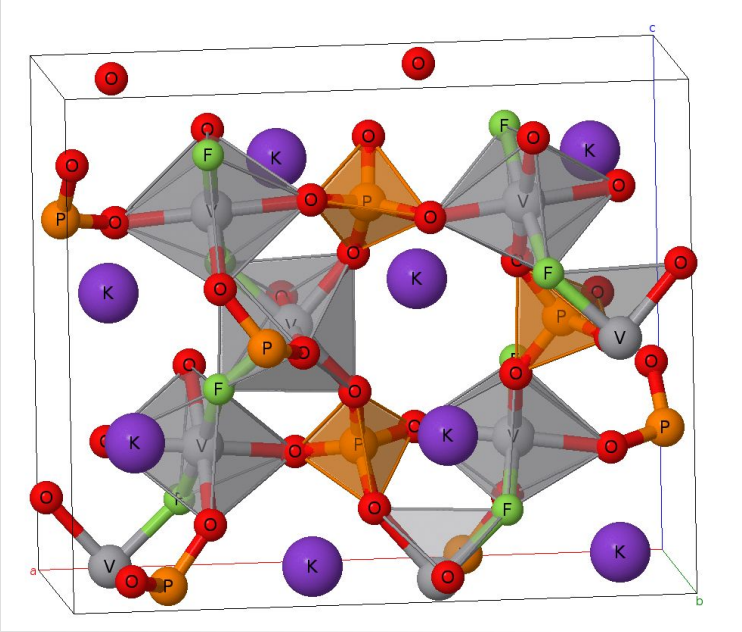

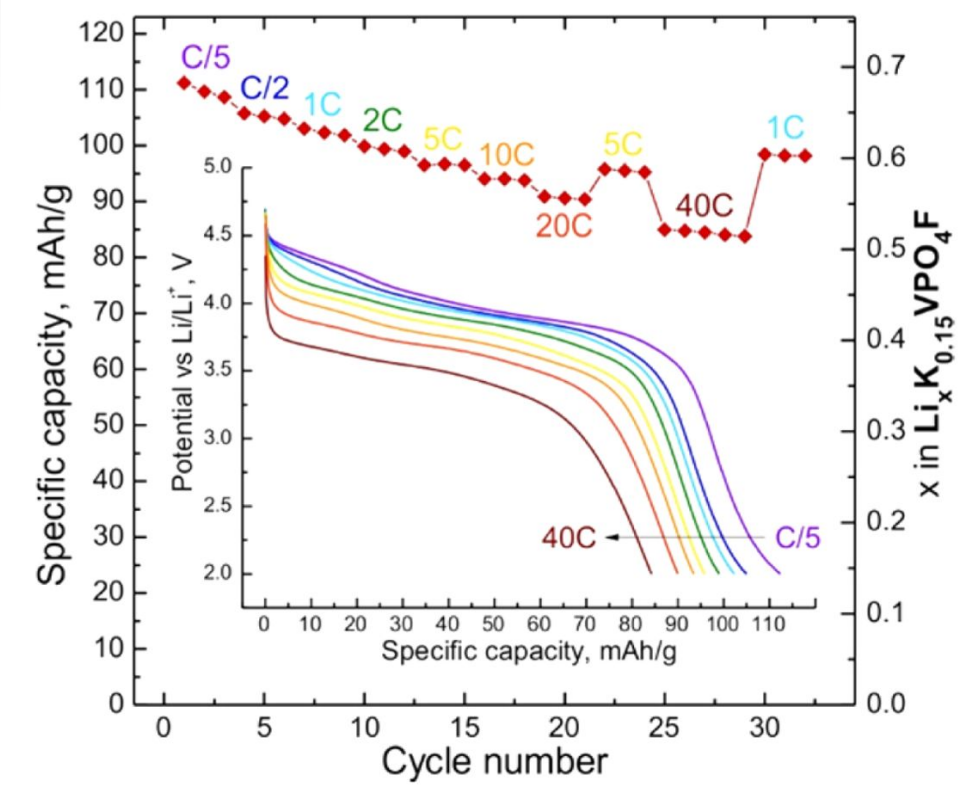

- Relatively low cost
- Possible intercalation of Li, Na, and K
- High intercalation voltage 4 V
- Very high specific rate

75 % of initial capacity at 40C

Fedotov, Stanislav S., et al. "AVPO4F (A= Li, K): a 4 V cathode material for high-power rechargeable batteries." *Chemistry of Materials* 28.2 (2016): 411-415.

Migration in $KVPO_4F$ (IS) and VPO_4F (DS)

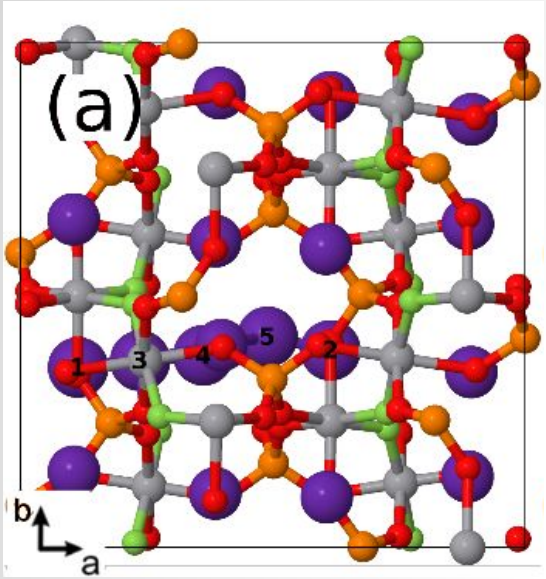

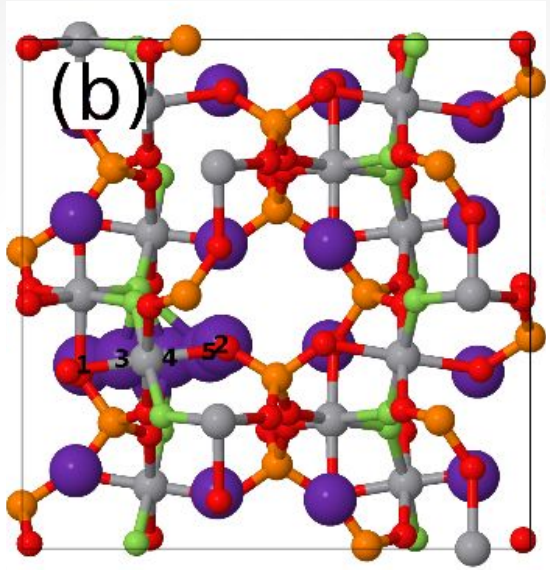

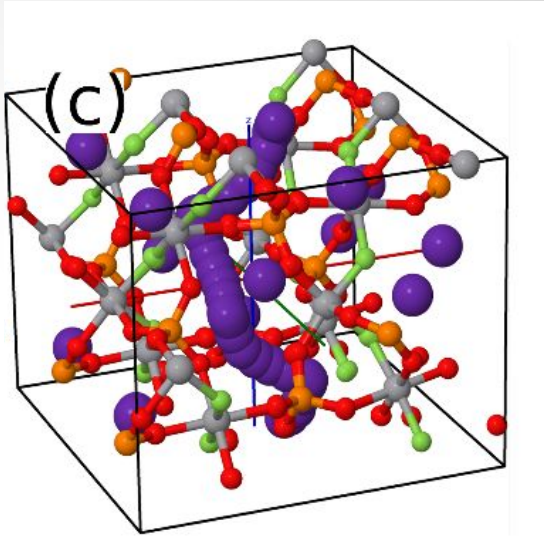

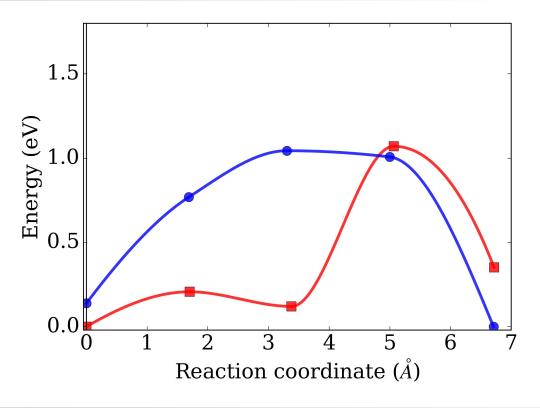

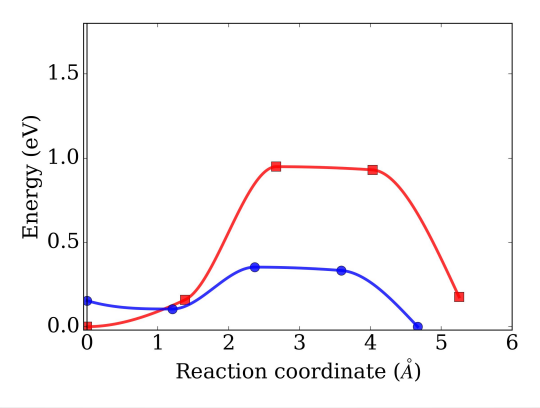

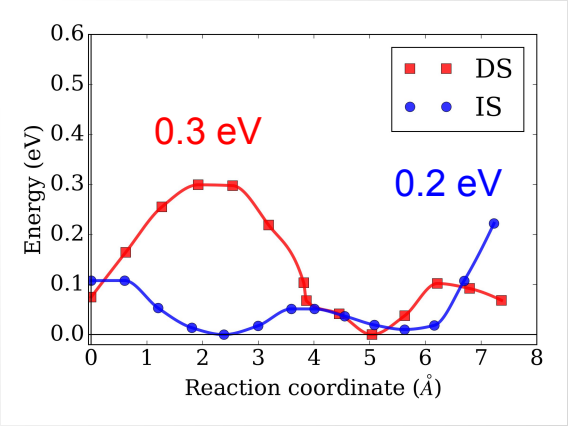

Fedotov, S. S., Samarin A.S., Nikitina V.N, **Aksyonov D.A.**, et al. // *Journal of Materials Chemistry A* 6, no. 29 (2018): 14420-14430.

NEB calculation in SIMAN

```
add_neb(st = st, it_new = 'LiFePO4', ise_new = '
    ion_relax', it_new_folder = 'LiFePO4/neb',
    images = 3)
```

```
res('LiFePO4.n3Li1v1', 'ion_relax', [1,2,3,4,5],
    show = 'fomepp', analys_type = 'neb'  )
```

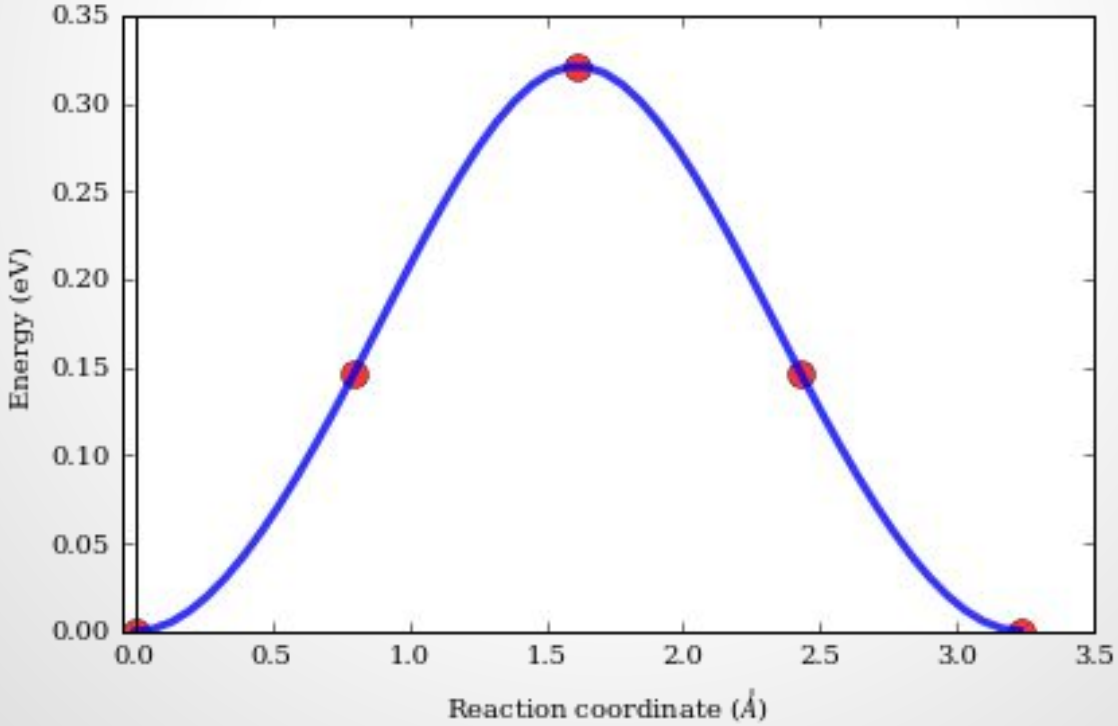

Three classes of cathodes are considered

Spinel, $LiMn_2O_4$

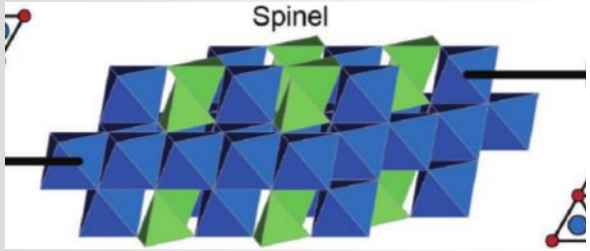

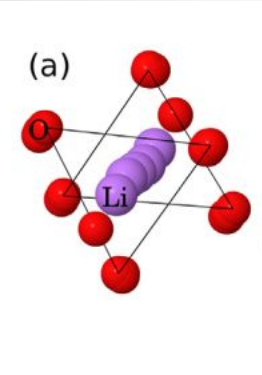

Olivine, $LiFePO_4$, $LiMnPO_4$

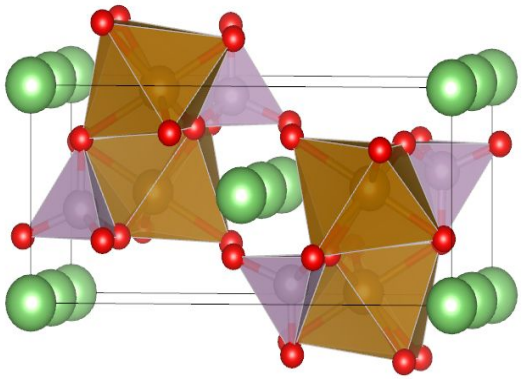

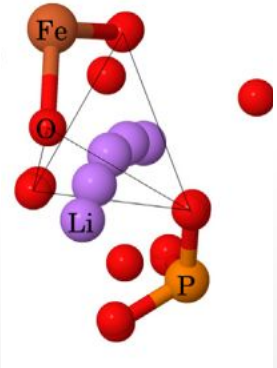

Tavorite, $LiVPO_4F$

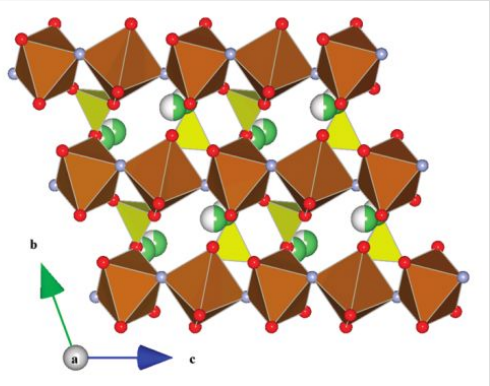

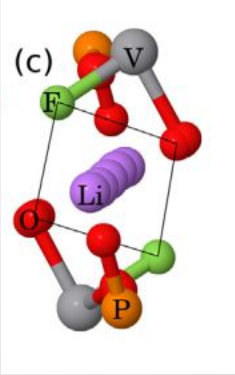

Origin of migration barriers

- What is the origin of migration barrier in cathode materials ?
- Is there any difference between Li, Na and K migration?

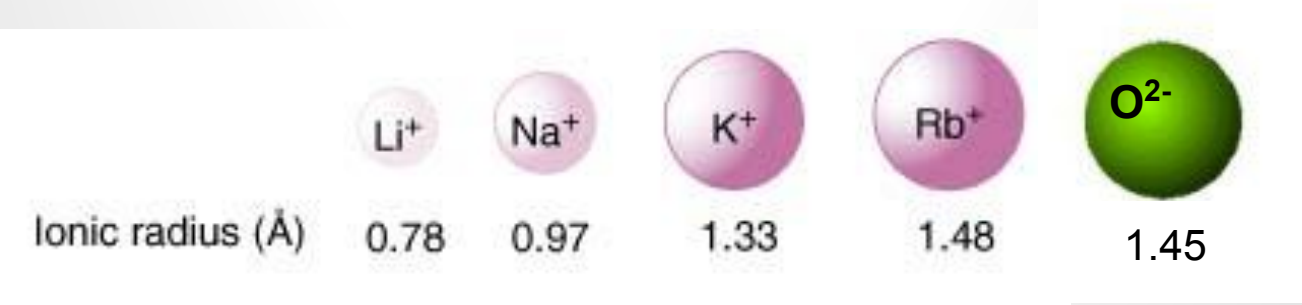

Migration barriers with NEB method

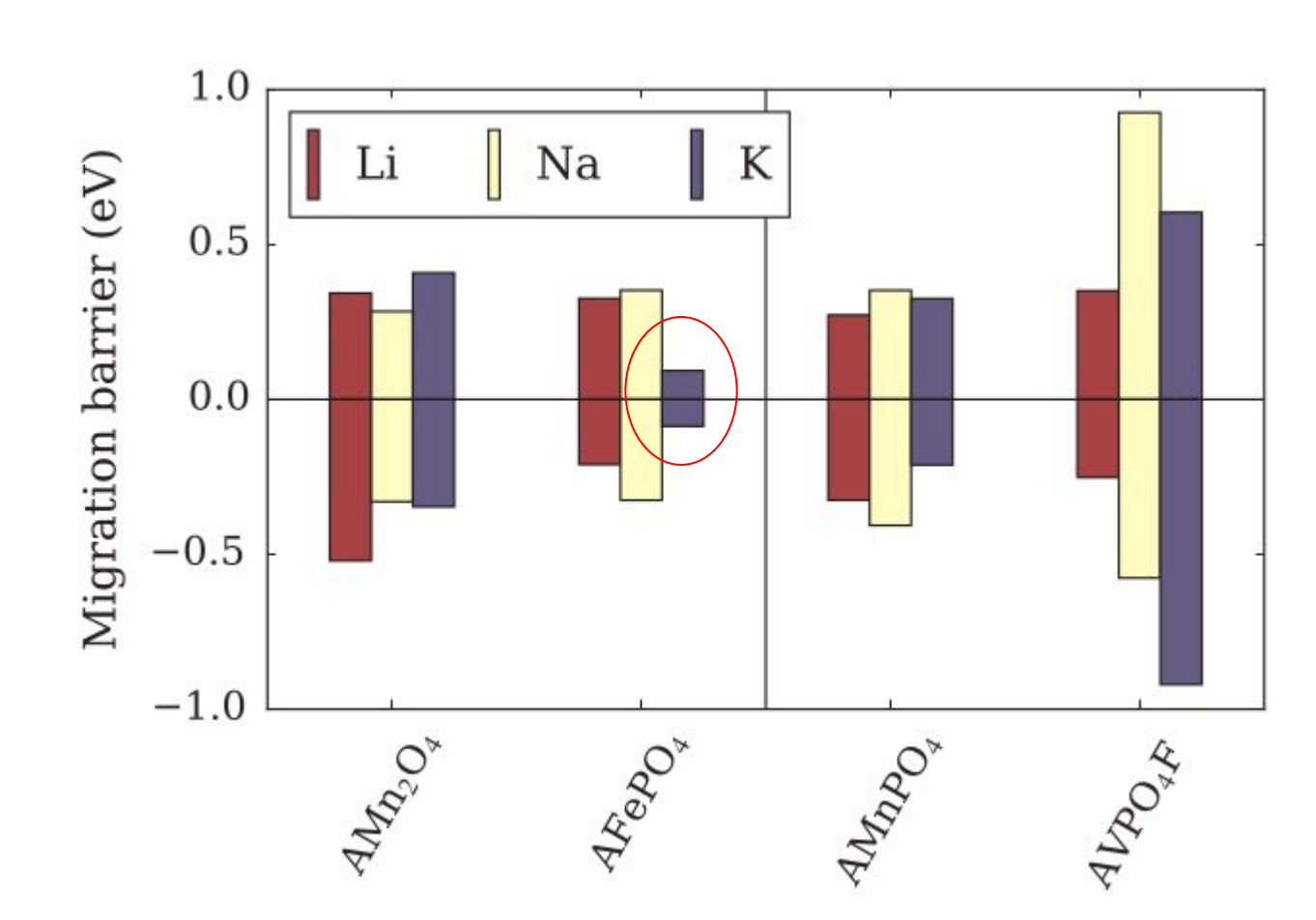

Intercalated state - Vacancy migration

Deintercalated state - interstitial migration

Local contributions to migration barrier

$$E_{DFT} = E_{site} + E_{lattice} \text{ - approximately}$$

$$E_{site} = \sum Z_i/R_i + \sum \lambda_i \exp(-R_i/\rho_i)$$

- R_i - distance between each cation and migrating cation
- site electrostatic energy based on effective charges and Ewald summation
- λ_i and ρ_i are parameters for short range Born-Mayer repulsive interaction [Kunz1992]

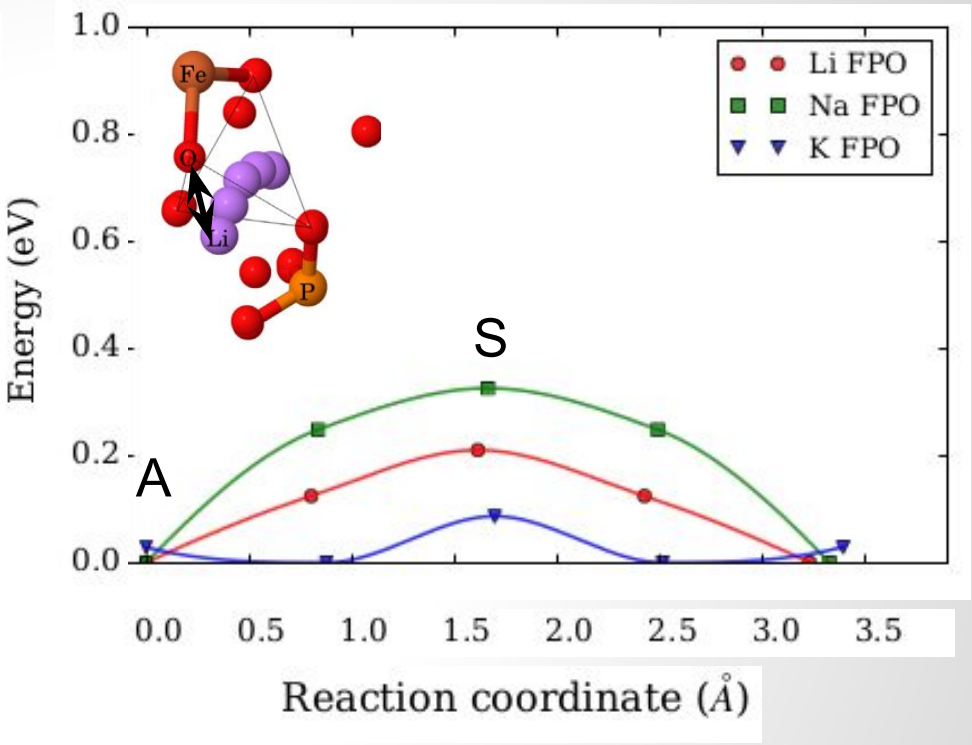

$$dE_{DFT} = E(S, DFT) - E(A, DFT)$$

$$dE_m = E_m(S) - E_m(A)$$

For many cases it is equivalent to migration barrier

Repulsive and electrostatic site energy

Change of repulsive energy vs dE(DFT)

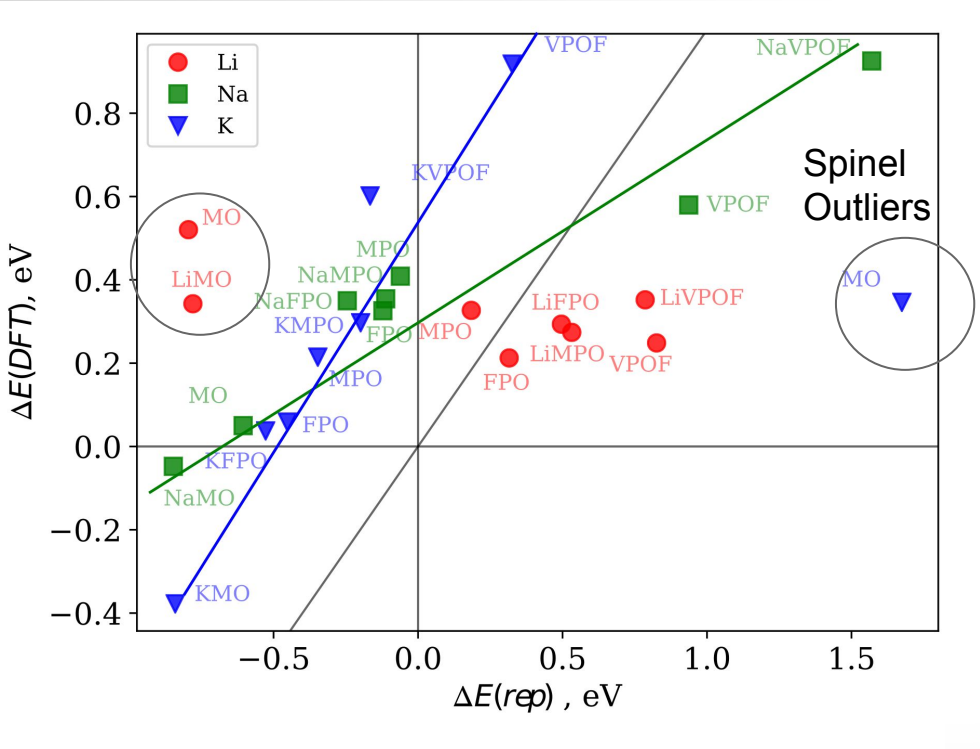

Change of ES energy vs dE(DFT)

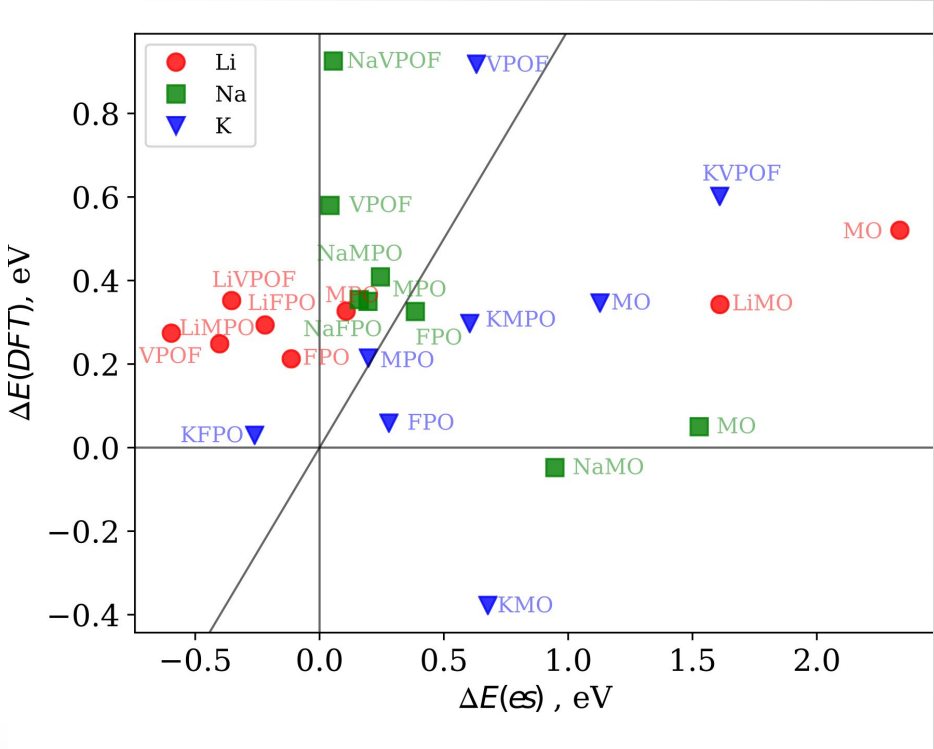

For K (MO omitted) and Na proportionality can be identified $R^2 = 0.6$

No correlation at all

Sum of repulsive and ES term vs dE (DFT)

$$\Delta E_{lattice} = \Delta E_{DFT} - \Delta E_{site}$$

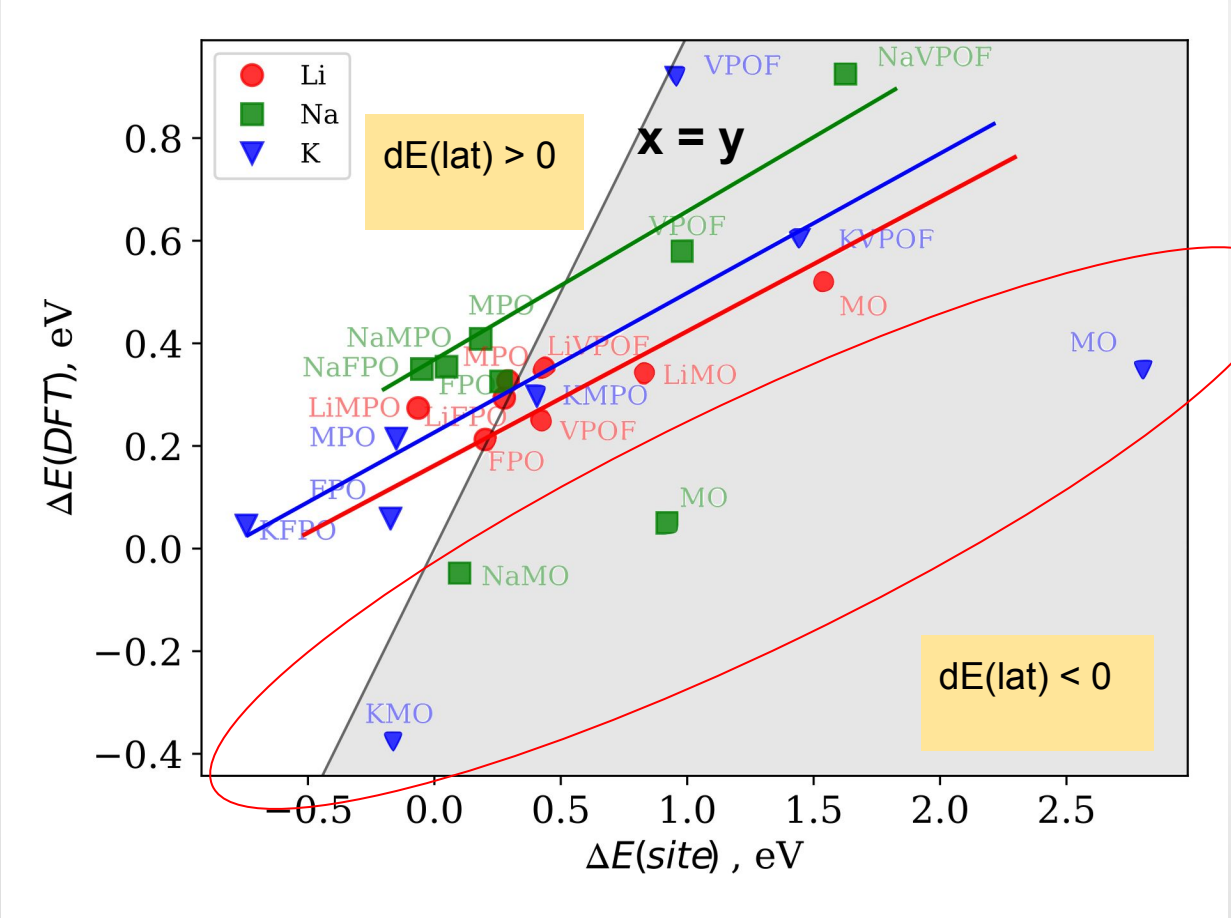

Classical Interatomic potentials, ΔE_{site} + $\Delta E_{lattice}$ (Pedone)

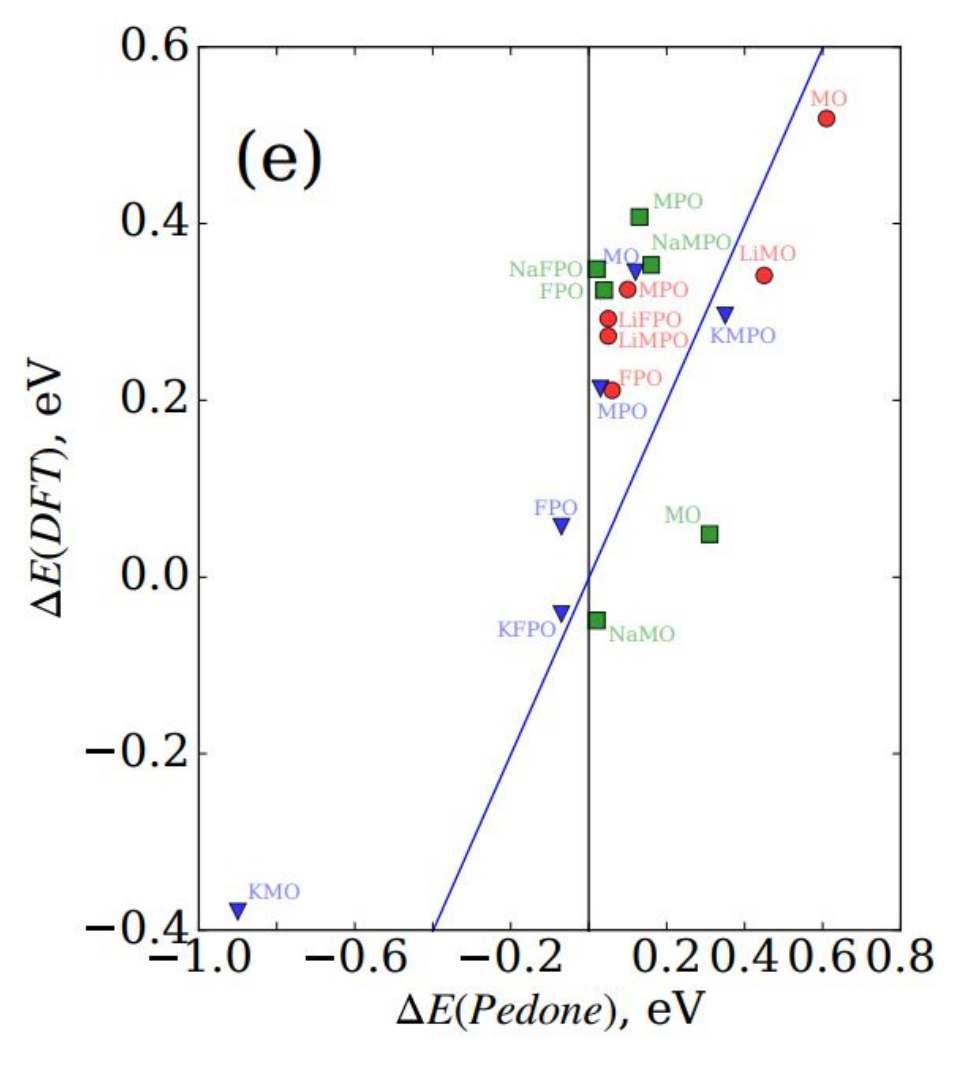

- Without potential parametrization, R^2 = 0.6
- Good quantitative description
- Spinel outliers are on line
- The lattice contribution is responsible for reducing energy at saddle point

Acknowledgments

PhD **A.Boev,**

Belgorod State University

Dr. **S.Fedotov,**

Skoltech

Prof.

A, Zhugayevych

Skoltech

Prof.

K.Stevenson,

Skoltech

Prof.

A.Abakumov,

Skoltech

Thank you for your attention!